

METHODS FOR DETERMINING SHEAR STRENGTH  
OF SOILS AND THE LIMITATIONS AND/OR  
ADVANTAGES OF THE VARIOUS TESTS

by

Amit Mukherjee

B.E., Calcutta University, India, 1983

---

A MASTER'S REPORT

submitted in partial fulfillment of the  
requirements for the degree


MASTER OF SCIENCE

Department of Civil Engineering

KANSAS STATE UNIVERSITY  
Manhattan, Kansas

1987

Approved by:

  
Wayne W. Williams  
Major Professor

## TABLE OF CONTENTS

	Page
LIST OF TABLES . . . . .	iv
LIST OF FIGURES . . . . .	v
CHAPTER 1. INTRODUCTION . . . . .	1
1.1 OVERVIEW . . . . .	1
1.2 PURPOSE AND SCOPE . . . . .	2
CHAPTER 2. LITERATURE REVIEW . . . . .	3
CHAPTER 3. DISCUSSION . . . . .	7
3.1 BASIC PRINCIPLES RELATING TO FRICTION BETWEEN SOLID BODIES . . . . .	7
3.2 TOTAL SHEARING STRENGTH OF SOIL . . . . .	11
3.3 SHEARING RESISTANCE AND STRENGTH . . . . .	12
3.4 COULOMB'S EQUATION . . . . .	15
3.5 PRINCIPLE OF EFFECTIVE STRESS . . . . .	18
3.6 MOHR THEORY OF FAILURE . . . . .	22
3.7 STRESS-STRAIN CHARACTERISTICS DURING SHEAR . . . . .	26
3.8 STRENGTH CHARACTERISTICS DURING SHEAR . . . . .	27
3.9 PORE PRESSURE PARAMETER A . . . . .	28
CHAPTER 4. SOIL TESTS . . . . .	33
4.1 SOIL CHARACTERISTICS AFFECTING SHEARING STRENGTH . . . . .	33

	Page
4.2 TESTS FOR MEASURING SHEAR PROPERTIES OF SOILS . . . . .	34
4.2.1 STANDARD PENETRATION TEST . . . . .	35
4.2.2 VANE SHEAR TEST . . . . .	37
4.2.3 THE 'DUTCH' CONE PENETROMETER TEST . . . . .	40
4.2.4 PRESSUREMETER . . . . .	41
4.2.5 DIRECT SHEAR TEST . . . . .	43
4.2.6 THE TRIAXIAL COMPRESSION TEST . . . . .	46
4.2.6.1 Principle of the Triaxial Compression Test . . . . .	52
4.2.6.2 Methods of Triaxial Testing . . . . .	56
4.2.6.3 Stress condition in specimen during Triaxial Compression Test . . . . .	58
4.2.6.4 Application of the Triaxial Test to the principle soil types . . . . .	59
4.2.6.4.1 Undrained tests on saturated cohesive soils . . . . .	60
4.2.6.4.2 Undrained tests on partly saturated cohesive soils . . . . .	61
4.2.6.4.3 Consolidated-undrained tests on saturated soils . . . . .	62
4.2.6.4.4 Drained tests . . . . .	63
4.2.7 UNCONFINED COMPRESSION TEST . . . . .	66

	Page
4.2.8 APPLICATION OF THE TRIAXIAL TEST TO THE SOLUTION OF ENGINEERING PROBLEMS . . . . .	69
4.2.8.1 Analysis in which pore pressure is an independent variable . . . .	69
4.2.8.2 Analysis in which pore pressure is a function of the stress change . . . . .	71
4.2.9 LIMITATIONS OF THE TRIAXIAL COMPRESSION TEST . . . . .	74
CHAPTER 5. CONCLUSIONS . . . . .	98
BIBLIOGRAPHY . . . . .	99
ACKNOWLEDGEMENTS . . . . .	101



LIST OF TABLES

Table No.		Page
4.1	Relation of Consistency of Clay, Number of Blows N on sampling Spoon, and Unconfined Compression Strength . . . . .	77
4.2	Sizes of Penetrometer needles . . .	77

## LIST OF FIGURES

Fig.No.		Page
3.1	(a,b,c) Friction on Horizontal Surface .	78
3.2	Modes of Failure in Soils 1-brittle failure, 2-deformation, 3-no proper deformation, 4-maximum failure load and ultimate values are different . . .	78
3.3	Shear Pattern a. Single Slip Line b. Family of Slip Lines . . . . .	78
3.4	Graph of Coulomb Formula for shearing strength of soils . . . . .	79
3.5	a. Relationship between major and minor principal stresses in the case of failure . . . . . b. Envelope of Mohr's circles: 1-5 = Mohr's circles . . . . .	79 79
3.6	Mohr Diagram for Normal and Shearing Stresses . . . . .	80
3.7	Graph of $\sigma_1 - \sigma_3$ vs. axial strain for undrained test on a compacted fill material . . .	80
3.8	Graph of volumetric strain vs. axial strain for undrained test on compacted fill material . . . . .	80
3.9	Stresses on a compressible, isotropic soil element . . . . .	81
3.10	Stress change stages in the Triaxial test. . . . .	81
4.1	Standard Split Barrel Sampler Assembly .	82
4.2	Relation between relative density, $\rho_r$ , and N obtained from the Standard Penetration Test . . . . .	82
4.3	Chart for correction of N values in sand for influence of overburden pressure . . .	83

Fig.No.		Page
4.4	Design chart for proportioning shallow footings on sand . . . . .	84
4.5	Relationship among Standard Penetration Resistance, relative density, and effective overburden pressure for coarse sand . .	85
4.6	a. Vane Shear Test Apparatus . . . . .	86
	b. Geometry of Field Vane . . . . .	86
4.7	Assumed distribution of shear stress on side surface and ends of soil cylinder in the Vane Shear Test . . . . .	86
4.8	Soil Penetrometer . . . . .	87
4.9	The Portotype Fugro Full Displacement Pressuremeter (FDPM) . . . . .	87
4.10	Set-up for prototype FDPM testing . . . . .	88
4.11	Direct Shear Stress Test Apparatus . . . . .	89
4.12	Schematic Diagram of the Direct Shear Test . . . . .	89
4.13	Failure envelope for clay obtained from the Direct Shear Test . . . . .	90
4.14	Direct Shear Test Methods:	
	a. Stress-control method . . . . .	90
	b. Strain-control method . . . . .	90
4.15	Schematic illustration of Triaxial Compression Cell . . . . .	91
4.16	Shear stress vs. normal compressive stress relationships for the three types of soils . . . . .	91
4.17	Graph of Coulomb Equation for shearing strength of soil . . . . .	92
4.18	Principle of the Triaxial Compression Test . . . . .	92

Fig.No.		Page
4.19	a. Physical representation of stressed sample . . . . .	93
	b. Mohr's circle representation of the same stressed sample . . . . .	93
4.20	Stress representation by p and q . . . . .	94
4.21	Stress condition and failure envelope generated from the Triaxial Compression Test . . . . .	95
4.22	Total stress Mohr's circles and failure envelope ( $\phi = 0$ ) obtained from unconsolidated-undrained triaxial tests . . . . .	95
4.23	Total stress failure envelope for undrained test on partly saturated cohesive soils . . . . .	96
4.24	Total and effective stress failure envelope for consolidated-undrained triaxial tests . . . . .	96
4.25	Effective stress failure envelope from drained tests in sand . . . . .	97
4.26	Failure envelope from Unconfined Compression Test . . . . .	97

## CHAPTER 1: INTRODUCTION

### 1.1 OVERVIEW

Shear strength, compressibility, shrink-swell behavior, and permeability are among the most important aspects of soil behavior in determining the suitability of soils for engineering purposes. Significant changes occur in the above-mentioned soil properties over time. This makes soils all the more difficult and interesting to work with. The engineer soon learns that soil is not inert but alive and sensitive to its environment.

In a laboratory test the specimen is intended and generally assumed to represent an undisturbed portion of soil at a single point in a soil medium. The validity of this assumption depends on the uniformity of the soil and of the stress and strain distributions within the soil samples. Separate measurements are often made for the soil phase, the water phase, and sometimes the air phase of the specimen in order to relate their individual contributions to the strength of the mass.

Two basic problems exist in present-day soil analysis. These are:

1. The effects of unloading the samples taken from depths below the surface as the sample is brought to the surface and removed from the sampler.

2. Changes in the moisture content that may occur in the soil strata after construction is complete and the effects these changes will have upon the strength and compressibility of the soil mass.

Simplistic soil tests such as the Standard Penetration Test, and the Vane Shear Test can only predict a shear value for the conditions at which the test is conducted.

## 1.2 PURPOSE AND SCOPE

It is the purpose of this report to discuss the various methods used for the determination of the shear strength of soil and the limitations and/or advantages of the various tests.

The scope of the paper is limited to a study of the existing literature with the author's interpretation based on experience and classwork at Kansas State University. The interested reader can refer to "The Measurement of Soil Properties in the Triaxial Test" by A.W. Bishop and D.J. Henkel for more details on the principles and development of the triaxial test over the years.

## CHAPTER 2: LITERATURE REVIEW

Although in-situ conditions are usually anisotropic, isotropic conditions were generally assumed in routine triaxial compression testing of naturally sedimented and compacted soils. The reason generally given for this testing inconsistency is that anisotropic conditions requires complicated procedures and extra periods of time. Tests measuring the stress-strain characteristics of anisotropically consolidated soils are very different from those determined on the same soil using isotropic consolidation.

Early investigations by Rendulic(16) indicated that the change in water content during consolidation and stress paths during shear are the same in consolidated undrained tests (CU) performed on both isotropically consolidated (ICU) specimens and anisotropically consolidated undrained (ACU) specimens, provided that the vertical consolidation stress  $\sigma_1$  is the same in both cases. This theory was emphasised by Taylor(1) and later confirmed by Henkel(1).

Based on this, Skempton and Bishop(1) assumed that the pore pressure parameter A at failure,  $A_f$ , and the effective angle of internal friction,  $\phi'$ , are constant and are

not influenced by the effective consolidation ratio,  $K_c$ , where  $K_c = \frac{\sigma_3}{\sigma_1}$  and  $\sigma_3$  is the lateral consolidation stress.

Rutledge(1) stated that the water content after consolidation and the undrained strength  $S_u$  are independent of  $K_c$ . Broms and Ratnam(1) verified the Rutledge hypothesis, but they based their conclusions on tests of compacted soils having liquid limit,  $LL = 55\%$  (prepared for testing by passing premoistened soil through a sample extruder). These tests showed that, apart from its dependence on  $K_c$ , the  $\frac{S_u}{\sigma_1}$  ratio for ACU specimens was also a function of the rate of strain during shear and also that  $A_f$  and the axial strain values at failure were lower for ACU than for ICU specimens. Whitman et al(1), testing a reconsolidated clay of  $LL = 63\%$  (prepared by consolidating a slurry in a large consolidometer), reported that the ratio  $\frac{S_u}{\sigma_1}$  may be independent of  $K_c$  when the specimen has been brought close to failure during consolidation. They also noted that for a given value of  $\sigma_1$ , water contents were higher in ACU than in ICU tests.

Donaghe and Townsend(1) conducted CU triaxial tests on clay specimens to test the Rutledge hypothesis. In order to simulate the response of naturally sedimented and consolidated materials, they trimmed the specimens from sam-



ples prepared by consolidating slurries of the material in large diameter consolidometers.

These experiments yielded the following results:

1. The ACU specimens had higher water contents (lower volume changes) than did ICU specimens for the same  $\sigma_1$ .
2. For any given  $\sigma_1$  value,  $(\sigma_1 - \sigma_3)_{max}$  generally decreased with decreasing values of  $K_c$ . Conversely, for any given water content,  $(\sigma_1 - \sigma_3)_{max}$  is greater for ACU than for ICU specimens.
3. Stress-strain characteristics were significantly affected by  $K_c$ . The axial strain values at  $(\sigma_1 - \sigma_3)_{max}$  generally decreased with decreasing values of  $K_c$ .
4. Induced pore pressures at  $(\sigma_1 - \sigma_3)_{max}$  decreased substantially with decreasing values of  $K_c$  ratios for a given  $\sigma_1$  value. Likewise,  $A_f$  values were considerably lower for ACU specimens.
5. Values of  $\phi'$  taken at  $(\sigma_1/\sigma_3)_{max}$  exhibit no effect of  $K_c$ .
6. However, values of  $\phi'$  taken at  $(\sigma_1 - \sigma_3)_{max}$  decrease when  $K_c$  is decreased from 1.0 to 0.67 and increase when  $K_c$  is decreased from 0.67 to 0.50.

Much work has been done on the development of true triaxial testing facilities of geologic type materials. This work has recently been given significant emphasis, not only because processes in nature are inherently three dimensional and should modelled as such, but also because the wide use of powerful numerical methods has enabled engineers and scientists to analyse structural and soil structure systems with complex three-dimensional

geometries. The solutions obtained through these methods are only as good as the description of the material properties, usually given in the form of strength, stress-strain relationships, time, and temperature-dependent behavior.

It has been recognised for a long time that the intermediate principal stress  $\sigma_2 (\sigma_1 \geq \sigma_2 \geq \sigma_3)$  has a pronounced influence on the strength and deformability of soils. However, the classical methods of analysis employing constitutive relations have been restricted to the two-dimensions containing the major and minor principal stresses only. The solutions have traditionally been conservative.

## CHAPTER 3: DISCUSSION

### 3.1 BASIC PRINCIPLES RELATING TO FRICTION BETWEEN SOLID BODIES (3)

Shear in soils is similar in many respects to the widely observed phenomenon of friction between solid bodies, although there are important differences between the two subjects. Imagine a brick resting on a horizontal table top, as shown in Fig. 3.1(a). The brick is in equilibrium under its own weight  $W$  and the equal and opposite reaction  $N$  provided by the table. Now, suppose that, as indicated in Fig. 3.1(b), a horizontal Force  $S_a$  is applied to the brick near the plane of contact between the brick and the table. If this force is relatively small, the brick will remain at rest and the applied horizontal force will be balanced by an equal and opposite force  $S_r$  in the plane of contact. This resisting force is developed as a result of roughness characteristics of the bottom of the brick and the table surface.

If the applied horizontal force is gradually increased, the resisting force will likewise increase, always being equal in magnitude and opposite in direction to the applied force. There is a limit, however, to the amount of resistance which can be developed at the plane of

contact; and, when the applied force equals or exceeds the maximum possible resistance, equilibrium will be destroyed and the brick will move along the table top. This movement or slippage is a shear failure. The applied horizontal force is a shearing force and the developed force is the friction or shearing resistance. The maximum shearing resistance which the materials are capable of developing is called the shearing strength.

When the shearing force is applied to the brick as in Fig. 3.1, the resultant  $R$  of the shearing force and the weight acts at an angle with the line of action of the force representing the weight, which in this case is normal to the shear plane. This angle, designated as  $\alpha$  in Fig. 3.1(b) is called the obliquity of the resultant or simply the obliquity angle. When the shearing force is increased to a value just equal to the shearing strength, that is, when sliding or failure is impending, the obliquity angle reaches its maximum value and is designated as  $\alpha_m$  as in Fig. 3.1(c). The forces that are applied normal and tangential to the shear plane are related to each other in accordance with the following equations:

$$\tan \alpha = \frac{S_a}{W} \quad (3.1)$$

$$S_a = W \tan \alpha \quad (3.2)$$

In a similar manner, the reaction  $N$  to the weight of the brick, which also acts normal to the shear plane, may be combined with the shearing resistance to obtain a resultant  $R'$  which makes an angle  $\phi_d$  with the normal. This angle  $\phi_d$  is called the developed friction angle; and it is equal to the obliquity angle  $\alpha$ , since the reaction is equal to the weight and the shearing resistance is equal to the applied shearing force. The angle  $\phi_d$  depends on the magnitude of the applied shearing force, as long as this force is not sufficient to cause shear failure. However, when the applied shearing force is large enough to cause failure, the shearing resistance has reached its maximum possible value for the particular materials involved. The angle  $\phi_d$  reaches its maximum value at failure and this maximum value is designated as  $\phi$ , as shown in Fig. 3.1(c). This limiting angle  $\phi$  is called the friction angle and constitutes a physical property of the materials, which in this case are the brick and the table top.

Likewise, if shear on an interior plane in a mass of soil is considered, the angle  $\phi$  is a property of the soil and the value of  $\tan \phi$  is called the coefficient of friction of the soil. This coefficient is here denoted by  $\mu$ .

The value of  $\tan \phi$  is equal to the shearing strength of the soil divided by the reaction normal to the shear plane. Also it is equal to the shearing stress at failure divided by the applied weight force per unit area normal to the shear plane.

Thus:

$$\tan \phi = \mu = \frac{S_n}{N} = \frac{S_a}{W} = \tan \alpha_m \quad (3.3)$$

For example, if the friction angle  $\phi$  of a cohesionless soil is given as  $20^\circ$ , it means that the soil is capable of providing sufficient shearing resistance to maintain equilibrium as long as the applied shearing force produces an angle  $\phi_a$  less than  $20^\circ$ . When the applied shearing force causes  $\phi_a$  to become equal to or greater than  $20^\circ$ , shear failure will result.

The preceding discussion indicates that shearing stress and strength attributable to friction can exist only under the following conditions. First, there must be a force normal to the plane on which shear is being considered; second, the material must exhibit friction characteristics, that is, it must have a finite coefficient or angle of friction. For example, if a quantity of clean, dry, cohesionless sand is poured out on a level surface, it will come to rest in a cone-shaped heap. The reason

sand can be piled up in this manner is because it has the property of internal friction. It has a definite value of the angle  $\phi$  and is in equilibrium at a definite angle of repose. In contrast to the sand, water has no shearing strength, and its angle  $\phi$  is zero. It flows freely downhill under the influence of gravity because of this fact. Furthermore, if a quantity of water is poured out on a level surface, it will spread out in a very thin layer and cannot be heaped up. Its angle of repose is zero.

### 3.2 TOTAL SHEARING STRENGTH OF SOIL (3)

Some soils have a finite shearing strength even when they are not subjected to external forces normal to a shear plane. Furthermore, when soils of this kind are subjected to normal forces, the shearing strength is not increased. These are called cohesive soils; and their shearing strength, which is independent of the normal pressure, is called cohesion or no-load shearing strength. Cohesion may be illustrated by considering two sheets of fly-paper with their sticky sides in contact. Considerable force is required to slide one sheet over the other, even though no normal pressure is applied. The



shearing resistance in this case is due to the cohesion between the sticky surfaces. In contrast to this, shearing resistance due to friction may be illustrated by considering two sheets of sand paper with their sanded surfaces in contact. These may be very easily caused to slide over each other when no normal force is applied. When a normal force is applied, the resistance to sliding or the shearing strength increases in direct proportion to the normal force.

### 3.3 SHEARING RESISTANCE AND STRENGTH (3)

One of the most important tasks in the application of soil mechanics to engineering problems is the study of soil behavior under load. In the design of structures the engineer relies upon the laws of applied mechanics and he determines the stresses and strains in the structural elements on the basis of a few physical characteristics of the construction materials used. Steel is unique in this respect in that it exhibits, within a well defined stress regime, such simple mechanical properties that permit a straightforward application of the theoretical analysis to practical problems. The same applies to soils. As far as soils are concerned, the theory of elasticity has a rather



limited scope. Therefore, problems of stability and strength such as bearing capacity, earth pressure on retaining walls, safe angle of slope, etc., are usually solved by limit-state stability analysis. This means that in the study of load-bearing capacity, we determine, regardless of the soil deformation, the ultimate pressure that causes a slip failure beneath the foundation, and the allowable soil pressure is then obtained by safety considerations. There is hardly a problem in the field of soil engineering which does not involve the shear properties of soil in the same manner.

The term shearing strength means the maximum resistance of soil to shearing stress. If external forces surpass this internal resistance, a failure occurs.

The strength of a material is rather difficult to define exactly, especially for soils. This difficulty arises from the many ways in which soils may fail. Failure may take the form of an abrupt brittle rupture or of a plastic flow with large and continuous deformations. Such differences in soil behavior are illustrated by typical stress-strain curves as in Fig. 3.2. Curve 1 represents a brittle failure with a definite ultimate strength value. In contrast to this, curve 2 exhibits no marked rupture value but it approaches a rather vaguely

defined vertical asymptote. Curve 3 does not even have a vertical asymptote, and failure cannot be defined at all. Curve 4 shows the case where the peak and ultimate strength values are different.

Failure itself may take place in two different ways. In the first instance failure conditions are satisfied only on a single surface known as surface of sliding or surface of rupture whereas the rest of the soil mass remains in the elastic state. In the second case an entire mass of soil, or a part of it bounded by a surface of sliding is in a state of rupture. Failure conditions prevail at every point within the mass, and at least two intersecting surfaces of sliding pass through every point. Refer Fig. 3.3.

The deformations of large soil masses are mainly due to the relative displacements between the particles. By strength of earth masses is, therefore, primarily meant the shearing strength. If only a single surface of sliding exists(a, Fig. 3.3), shear deformations are confined to that surface. In the second case(b, Fig.3.3) deformations develop within the entire mass in the state of rupture. Shearing strength was previously defined as the ultimate shearing stress on the surface of sliding. For the second case of failure, however, this surface is

difficult to exactly define, and failure criteria must therefore be given in terms of the principal stresses that can yet be mobilized.

### 3.4 COULOMB'S EQUATION (3)

Most natural soils exhibit shearing resistance due to both cohesion and friction. These components of strength are found to exist in widely varying relationships, ranging from zero cohesion in the case of clean, dry sand to practically zero friction in the case of fine grained, highly plastic clay. The cohesion and friction components are added together to give the total shearing strength properties of the soil. The shearing strength is expressed by an empirical formula proposed by Coulomb. This formula is:

$$S = c + N \tan \phi \quad (3.4)$$

in which,

S = shearing strength  
c = cohesion  
N = pressure normal to shear plane  
 $\phi$  = friction angle of soil  
 $\tan \phi = \mu$  = coefficient of friction

The Coulomb formula is an equation for a straight line having an intercept on one coordinate axis. A typical graph of the equation is shown in Fig. 3.4. in which unit

pressures normal to a shear plane are plotted as abscissas and unit shearing stresses are plotted as ordinates. The intercept at zero pressure represents the cohesion of the soil, and the angle which the graph makes with the horizontal is the friction angle  $\phi$ . A graph of this kind is called a shear diagram. If the graph is extended to the left of the origin and the graph is prolonged to intersect the horizontal axis, the distance from this point of intersection to the origin may be thought of as an internal initial stress which is inherent in the material and is associated with the cohesion property. It is analogous to molecular attraction in solid particles.

The correct definition of shearing strength of soil is one of the most difficult problems in soil mechanics. A part of this difficulty arises from the fact that shearing strength is not an intrinsic property of a given soil, but varies over a considerable range with varying conditions, such as density, moisture content, and degree of consolidation. This fact dictates the necessity of testing the soil in the worst probable condition in which it will exist in the prototype soil mass that the test sample represents. It is sometimes difficult to predict this worst probable condition, and it is also difficult to duplicate the condition in the test. Further difficulties

arise from the usual non-homogeneity of the soil masses and the consequent uncertainty of obtaining representative samples for testing. Moreover, the available methods of shear testing require rigorous techniques. Nevertheless, it is incumbent upon a soil engineer to make every possible effort to obtain adequate and precise information concerning the shearing strength of the soil, commensurate with the nature and importance of the problem with which he is associated.

### 3.5 PRINCIPLE OF EFFECTIVE STRESS (1)

Triaxial tests can be run with or without the measurement of pore water pressures. If pore water pressures are not measured, the evaluation of shear strength properties is on a total stress basis. With the measurement of pore water pressures, the data can be evaluated on an effective stress basis. It is always preferable to evaluate shear strength characteristics on an effective stress basis since this provides a better understanding of the processes taking place within the soil specimen. If for some reason it is not possible to measure pore water pressures, a total stress analysis can be used; but the laboratory testing should be such as to simulate the loading conditions in the field. Volume change measurements are very helpful with regard to the evaluation of the triaxial test data. Such measurements can easily be made on fully saturated samples of soil but are difficult on partially saturated and dry samples. However, for the optimum solution, triaxial tests should be conducted in such a manner that measurements of pore pressure and volume change are made in addition to the normal additions of loads and deformations to which the samples are subjected.

The strength and deformation characteristics of soil

are best understood by visualising it as a compressible skeleton of solid particles including voids which, in saturated soil, are filled with water, or, in partly saturated soil, with both air and water. Shear stresses can of course be carried only by the skeleton of solid particles. On the other hand, the normal stress on any plane is, in general, the sum of two components - the stress carried by the solid particles and the pressure in the fluid in the void space.

This, from the practical point of view, has two important consequences:

1. In the relationship between normal stress and volume change, the controlling factor is not the total normal stress, but the difference between the total normal stress and the pressure of the fluid in the void space, termed the pore pressure  $u$ . For an equal all-round change in stress, this is expressed quantitatively by the relationship:

$$\frac{\Delta V}{V} = -C_c (\Delta\sigma - \Delta u) \quad (3.5)$$

where

$\frac{\Delta V}{V}$  = change in volume per unit volume of soil,

$\Delta\sigma$  = change in total normal stress,

$\Delta u$  = change in pore pressure, and

$C_c$  = compressibility of the soil skeleton

The difference  $\sigma - u$  is termed the effective stress and denoted by the symbol  $\sigma'$ . This relationship may be illustrated as follows: a volume change will occur, without any change in the applied or total stress, if the pore pressure undergoes a change. This is the primary cause of the long-term settlements of buildings founded on clay, in which the excess pore pressure set up during construction dissipates only at a



slow rate. It also explains the additional settlement caused by ground water lowering, either for construction work or for water supply.

2. The shear strength of soil is largely determined by the frictional forces arising during slip at the contacts between the soil particles. These are clearly a function of the component of normal stress carried by the soil skeleton rather than of the total normal stress.

For practical purposes, therefore, the Coulomb equation may be modified into:

$$S = c' + (\sigma - u) \tan \phi' \quad (3.6)$$

where

$c'$  = apparent cohesion,  
 $\phi'$  = angle of shearing resistance,

(the above two parameters are in terms of effective stress.)

$\sigma$  = total pressure normal to the plane considered, and  
 $u$  = pore pressure

In most engineering problems relating to stability, the magnitude of the total normal stress on a potential slip surface may be reasonably estimated from statics considerations. On the other hand, the magnitude of the pore pressure is influenced by several factors. These include the following:

1. In the case of stationary ground water, the magnitude of the pore pressure is determined by the position of the element of soil under consideration, relative to the ground water level. Where approximately steady seepage exists (for example, in natural slopes; and in cuts and earth dams after the influence of the pore-pressure changes has died out) the pore pressure



is obtained from the flow net corresponding to the known boundary conditions.

The pore pressure is thus an independent variable and its magnitude is not related to that of the total normal stress. The function of the triaxial test is simply to obtain the relationship between shear strength and effective normal stress.

2. A change either in the normal stress or in the shear stress carried by the solid skeleton of the soil results in a tendency for volume change to occur within the soil mass. Unless the conditions for drainage are such that the fluid in the pore space can be freely expelled, an excess pore pressure will temporarily result from the stress change. The rate at which this excess pore pressure will dissipate depends principally on the permeability of the soil. During this period the pore pressure is a function of:
  - i. the initial stress change,
  - ii. the coefficient of consolidation, and
  - iii. the distance of the soil element from a surface at which drainage can occur.

In such cases the laboratory test may be called on to provide data not only on the relationship between shear strength and effective stress, but also on the initial pore pressure set up by a change in stress.

The use of the principle of effective stress in stability analysis thus involves two steps; first, the determination of shear strength parameters  $c'$  and  $\phi'$  and, second, the prediction of pore pressure at the most critical stage either of construction, operation, or long-term stability.

### 3.6 MOHR THEORY OF FAILURE (5)

External loads in a solid body induce induce internal stresses. When these stresses are increased to a sufficient extent, they overcome the internal resistance of the material thereby inducing failure, i.e., the body actually ruptures or else it undergoes very large permanent deformations. The stress at which failure occurs is referred to as limiting stress. It is, of course, the combined effect of all stress components acting at a given point that produces failure conditions. However, one is often faced with almost insurmountable difficulties to exactly simulate actual and often very complex stress conditions experimentally. It has therefore become necessary to determine strength conditions by relatively simple tests and, using the results obtained, predict the behavior of materials subject to composite states of stress by theoretical means.

Various theories have been developed relative to the stress condition in engineering materials at the time of failure. Each explains satisfactorily the actions of certain kinds of material at the time they fail but no one of them is applicable to all materials. The failure of a soil mass is more nearly in accordance with the tenets of the Mohr Theory of failure than with those of any other

theory, and the interpretation of the data of the triaxial compression test depends to a large extent on this fact.

Failure conditions may be expressed, in a general way, as a functional relationship between the three principal stresses:

$$f(\sigma_1, \sigma_2, \sigma_3) = 0 \quad (3.7)$$

Mohr's condition (5) defines the limiting condition as follows. If the Mohr circles are plotted to represent states of stress at failure, a common envelope can be drawn to these circles. Its shape depends upon the material. Supposing a Mohr circle intersects the Mohr envelope, it would mean that the corresponding state of stress is beyond the limiting state, but this is impossible. A Mohr circle, in turn, that lies entirely below the envelope indicates that failure condition has not yet been reached. An essential assumption in the Mohr failure theory is that the failure condition is independent of the intermediate principal stress. Hence Eqn. 3.7 reduces to:

$$f(\sigma_1, \sigma_3) = 0 \quad (3.8)$$

If we adopt the Mohr representation of state of stress, then Eqn. 3.8 gives the equation of the Mohr envelope.

It may be written in the form:

$$\tau = f(\sigma) \quad (3.9)$$

The two expressions for failure condition (Eqns. 3.8 & 3.8) are shown diagrammatically in Fig. 3.5. In soil mechanics a simplified form of the Mohr failure theory is used, which assumes, after Coulomb, that the failure relationship  $\tau = f(\sigma)$  is linear.

According to the Mohr Theory, as in Fig. 3.6, a material fails along the plane and at the time at which a certain optimum combination of normal stress and shearing stress occurs within a stressed body. This optimum combination of stresses is that which produces the maximum obliquity  $\alpha_m$  of the resultant of the normal and shearing stresses. In the Mohr diagram, the normal stresses are drawn as abscissas and the shearing stresses as ordinates. According to the Mohr Theory, the maximum obliquity  $\alpha_m$  is equal to the friction angle  $\phi$ . The value of the obliquity angle  $\alpha$  can never exceed  $\alpha_m = \phi$  without the occurrence of failure.

Normal and shearing stresses which yield plotted points below the envelope represent stress situations which do not produce failure. Points above the envelope do not exist, since the material will fail before such combinations of stresses can develop. In the case of cohesionless soils, the envelope passes through the origin representing applied stresses. For cohesive soils, the

envelope passes through the origin of total stress( initial plus applied ), and the ordinate for an applied stress equal to zero represents the value of shearing strength which is the cohesion of the soil. The principal objective, therefore, of a triaxial compression test is to establish the Mohr Envelope for the soil being tested.

It is interesting to note that the chord of a Mohr circle representing the stress situation at failure, which extends from the abscissa  $\sigma_3$  on the horizontal diameter to the point of tangency of the Mohr Envelope, is oriented so as to be parallel to the failure plane in the material. The angle between this chord and the horizontal axis represents the angle between the failure plane and the maximum principal plane, which is a horizontal plane in the triaxial test specimen. Therefore, when a specimen fails in such a manner that the shear-failure plane can be identified, the angle which it makes with the horizontal should be measured and compared with the angle between the chord and the horizontal on the Mohr diagram as a check on the results.

The Mohr failure theory represents only one of the general methods of defining the state of failure. It is based on the assumption that failure occurs solely due to slip. Failure is assumed to be independent of the defor-

mation characteristics and the Poisson number of the material. These are the essential features that make the Mohr theory particularly suited to the study of soil strength.

In the light of recent research, Mohr's concept does certainly not mean the last word in strength theory, and in many problems, it has proved inadequate in describing the true behavior of materials. Yet, for engineering purposes, it has become a very useful and dependable tool in judging, by strength computations, the danger of failure in solid bodies under general stress conditions.

### 3.7 STRESS-STRAIN CHARACTERISTICS DURING SHEAR (1)

The stress-strain plots obtained from the triaxial compression tests reveal the influence of relative density and strain conditions on the stress-strain characteristics of the soil tested. An increase in the initial relative density increased the initial slope of the stress difference  $\sigma_1 - \sigma_3$  versus the axial strain  $\epsilon_1$ , and also increased the strength of the material, as in Fig. 3.7. However, the axial strain at failure was found to decrease with increasing relative density.

The effect of the initial relative density on the volumetric behavior of the soil indicates that the



triaxial compression specimens exhibited compressional volumetric strain at the early stages of shear, as in Fig. 3.8.

However, specimens with low relative densities continued to compress, while those with high relative densities expanded with increasing axial strain. Specimens with intermediate relative density indicated intermediate volumetric strain during shear.

### 3.8 STRENGTH CHARACTERISTICS DURING SHEAR (1)

The Mohr-Coulomb Theory is used in evaluating the strength parameter  $\phi'$  on the assumption that the failure envelope is a straight line passing through the origin and that the theory is applicable to soil under plane strain shear deformation. Thus, the effective angle of internal friction may be defined as:

$$\phi' = \sin^{-1} \left( \frac{\sigma_1' - \sigma_3'}{\sigma_1' + \sigma_3'} \right) \quad (3.10)$$

A correlation between  $\phi'$  and the initial relative density showed that the angle  $\phi'$  increased almost linearly with increasing relative density. Taylor, while conducting direct shear tests, suggested that an amount of energy may be absorbed or generated during volume change which should be taken into account. Skempton and

Bishop(1) adopted this concept and derived an expression for correcting observed triaxial compression test data. The energy correction may be stated quantitatively as follows:

$$\Delta(\sigma_1 - \sigma_3) = \frac{\sigma_3'}{V_c} = \frac{d(\Delta V)}{d\epsilon_1} \quad (3.11)$$

where

$\Delta(\sigma_1 - \sigma_3)$  = amount of deviation in the observed stress difference

$V_c$  = initial volume

$\Delta V$  = change in volume, and

$\epsilon_1$  = axial strain.

### 3.9 PORE PRESSURE PARAMETER A (1)

The change in the pore pressure due to a change in the applied stress, during an undrained shear, may be explained in terms of empirical coefficients called the pore pressure parameters. A pore pressure parameter may be defined as a dimensionless number that indicates the fraction of the total stress increment that shows up an excess pore pressure for the condition of no drainage.

Consider the case in which the compressible skeleton of soil particle, as shown in Fig. 3.9, behaves as an elastic isotropic material and the fluid in the pore space shows a linear relationship between volume change and



stress. An increase in the three principal stresses will result in a decrease in volume of  $-\Delta V$  (where  $V$  is the initial volume) and a consequent increase in pore pressure of  $\Delta u$ . The increase in effective stress will thus be:

$$\Delta\sigma_1' = \Delta\sigma_1 - \Delta u, \quad \Delta\sigma_2' = \Delta\sigma_2 - \Delta u, \quad \Delta\sigma_3' = \Delta\sigma_3 - \Delta u \quad (3.12)$$

If  $\epsilon_1$ ,  $\epsilon_2$ , and  $\epsilon_3$  denote the strains in the three directions, we have:

$$E\epsilon_1 = \Delta\sigma_1' - \mu(\Delta\sigma_2' + \Delta\sigma_3')$$

$$E\epsilon_2 = \Delta\sigma_2' - \mu(\Delta\sigma_3' + \Delta\sigma_1')$$

$$E\epsilon_3 = \Delta\sigma_3' - \mu(\Delta\sigma_1' + \Delta\sigma_2') \quad \text{and,}$$

$$E(\epsilon_1 + \epsilon_2 + \epsilon_3) = E\epsilon_v = E \frac{\Delta V}{V} = (1-2\mu)(\Delta\sigma_1' + \Delta\sigma_2' + \Delta\sigma_3')$$

Decrease in volume of the soil skeleton is then:

$$-\Delta V = V \cdot \frac{1-2\mu}{E} \left\{ \Delta\sigma_1' + \Delta\sigma_2' + \Delta\sigma_3' \right\} \quad (3.13)$$

where

$E$  = Young's Modulus

$\mu$  = Poisson's ratio with respect to change in effective stress.

Decrease in volume of the soil skeleton is almost entirely due to a decrease in the volume of voids. If  $n$  is the initial porosity,  $C_w$  the compressibility of the fluid in the pore space, the volume change is as a result related to the pore pressure change, if no drainage occurs. Hence:

$$-\Delta V = n \cdot V \cdot C_w \cdot \Delta u \quad (3.14)$$

$$n \cdot C_w \cdot \Delta u = \frac{-\Delta V}{V} = \frac{1-2\mu}{E} \left\{ \Delta\sigma_1' + \Delta\sigma_2' + \Delta\sigma_3' \right\} \quad (3.15)$$

In the common type of triaxial test, the stress changes are made in two stages:

1. an increase in cell pressure resulting in an equal allround change in stress, and
2. an increase in axial load resulting in a change in the deviator stress.

If  $\Delta u_1$  is the change in the pore pressure during the first stage of the test when the cell pressure is applied, and  $\Delta u_2$  is the change in the pore pressure when the deviator stress is applied, then  $\Delta u = \Delta u_1 + \Delta u_2$

Under these conditions, changes in minor and intermediate principal stresses ( $\Delta\sigma_3$  and  $\Delta\sigma_2$  respectively) are both equal to the cell pressure, the increase in deviator stress being equal to  $\Delta\sigma_1 - \Delta\sigma_3$ . Putting  $\Delta\sigma_3 = \Delta\sigma_2$  in the above equations leads to the expression for  $\Delta u$  which may be arranged into terms representing change in cell pressure  $\Delta\sigma_3$  and a subsequent change in the deviator stress  $\Delta\sigma_1 - \Delta\sigma_3$ . Hence:

$$\Delta u = \frac{1}{1+n(c_w/c_c)} \left[ \Delta\sigma_3 + \frac{1}{3}(\Delta\sigma_1 - \Delta\sigma_3) \right] \quad (3.16)$$

where

$$c_c = \frac{3(1-2\mu)}{E}, \text{ the compressibility of the soil skeleton.}$$

This equation for soil under undrained conditions can be simplified into:

$$\Delta u = B \left[ \Delta\sigma_3 + A(\Delta\sigma_1 - \Delta\sigma_3) \right] \quad (3.17)$$

where  $B = \frac{1}{1+n(c_w/c_c)}$

This is the general equation for a single fluid for the change in pore pressure when a change in allround pressure is accompanied by a change in the deviator stress.

For a partially saturated soil with two fluids, we have:

$$\Delta u_w = B_w [\Delta \sigma_3 + A_w (\Delta \sigma_1 - \Delta \sigma_3)] \quad (3.18)$$

$$\Delta u_a = B_a [\Delta \sigma_3 + A_a (\Delta \sigma_1 - \Delta \sigma_3)] \quad (3.19)$$

For fully saturated soils, the value of  $C_w$  - that of water alone - is so small that  $B \approx 1$ . The value of  $A$  depends very largely on whether the soil is normally or overconsolidated, and on the proportion of the failure stress applied.

In the case of partly saturated soils, the value of  $B$  is much higher due to the presence of air in the pore space. The value of  $B$  is less than 1 but varies with the stress change. As a result, the value of  $B$ , which applies during the application of the deviator stress  $\Delta \sigma_1 - \Delta \sigma_3$  is different from the value applied during increase in allround stress  $\Delta \sigma_3$ .

Therefore it is convenient to express the Skempton equation as:

$$\Delta u = B \cdot \Delta \sigma_3 + \bar{A} (\Delta \sigma_1 - \Delta \sigma_3) \quad (3.20)$$

where

$$\bar{A} = A \cdot B = \frac{\Delta u}{\Delta \sigma_1 - \Delta \sigma_3} \quad (3.21)$$

For a fully saturated soil,  $B = 1$ , hence:

$$\Delta u = \Delta \sigma_3 + A(\Delta \sigma_1 - \Delta \sigma_3) \quad (3.22)$$

whence

$$A = \frac{\Delta u - \Delta \sigma_3}{\Delta \sigma_1 - \Delta \sigma_3} \quad (3.23)$$

For the usual undrained triaxial test where  $\Delta \sigma_3 = 0$

$$A = \Delta u / \Delta \sigma_1 \quad (3.24)$$

## CHAPTER 4: SOIL TESTS

### 4.1 SOIL CHARACTERISTICS AFFECTING SHEARING STRENGTH

When soil is loaded, shearing stresses are induced in it. When the shearing stresses reach a limiting value, shear deformation takes place, leading to the failure of the soil mass. The failure may be in the form of sinking of a footing, or movement of a wedge of soil behind a retaining wall forcing it to move out, etc. The stability of structures built on soil depend upon the shearing resistance offered by the soil along the probable surfaces of slippage. All stability analysis in soil mechanics involve a basic knowledge of the shearing properties and shearing resistance of the soil.

The shearing resistance of a soil is constituted basically of the following components:

1. the structural resistance or displacement of the soil because of the interlocking of the particles,
2. the frictional resistance to translocation between the individual soil particles at their contact points, and
3. cohesion or adhesion between the surface of the soil particles.

#### 4.2 TESTS FOR MEASURING SHEAR PROPERTIES OF SOILS (1)

The measurement of shear strength of soil involves certain test observations at failure with the help of which the failure envelope can be plotted corresponding to a given set of conditions. Shearing resistance can be determined by the following methods:

1. Direct Shear Test
2. The Triaxial Compression Test
3. Unconfined Compression Test

It is almost impossible to obtain satisfactory undisturbed samples of soft sensitive clays or of coarse granular soils, since even the most sophisticated sampling techniques cause excessive disturbance of these soils. Methods have therefore been devised for estimating the soil properties from the results of these tests carried out in-situ. A considerable number of such tests have been developed, of which the most important are:

1. The Standard Penetration Test
2. The Vane Shear Test
3. The 'Dutch' Static Cone Penetrometer
4. The Pressuremeter

Again, depending upon the drainage conditions, three types of shear tests have been developed:

1. undrained or quick test
2. consolidated-undrained test
3. drained test

The parameters  $c$  and  $\phi$  are not fundamental properties of the soil; they may simply be considered coefficients derived from the geometry of the graph obtained by plotting shear stress at failure against normal stress. They vary with drainage conditions of the test.

#### 4.2.1 THE STANDARD PENETRATION TEST (10, 24) (ASTM Standard D 1586-67(1974))

The usage of this test method for soil analysis was formalized and given credibility to by Terzaghi and Peck (24) in 1947. In this method the blow count or N value was related to the bearing capacity of soils in several ways. This test has been used extensively in the US and in Britain for estimating the relative density and angle of shearing resistance of coarse granular soils. A standard split spoon sampler, about 50 mm. in diameter (Fig. 4.1), is driven into the ground by blows from a drop hammer weighing 64 kg.(140 lb.) and falling 0.76 m.(30 in.). The sampler is driven 0.15 m.(6 in.) into the soil at the bottom of the borehole and the number of blows (N) required to drive it a further 0.3 m.(12 in.)

is then recorded.

Although this test is entirely empirical, considerable experience with its use has enabled a reasonably reliable correlation to be established between the N value and certain soil properties. Fig. 4.2 shows Peck, Hansen and Thornburn's relationship between N and the relative density and the angle of shearing resistance  $\phi$ .

Table 4.1 shows what Terzaghi and Peck perceived the approximate relationship between blow count N and the unconfined compressive strength of the clay stratum to be.

The usage of the N value for evaluating soil bearing capacity was changed by Peck, Hansen and Thornburn in 1953 with the introduction of a correcting factor for the N value with regard to the amount of the overburden effective stress. See Fig. 4.3.

The basic correction formula is

$$C_N = 0.77 \log_{10} \frac{20}{\sigma_e} \quad (4.1)$$

where

$C_N$  = corrected N value to use for design but never greater than 2.0

$\sigma_e$  = effective overburden pressure at depth of sampling (in tons per sq.ft.)

Peck, Hansen and Thornburn (10) presented the general chart for blow count N and bearing capacity in a different



form as shown in Fig. 4.4.

Hough (24) related the blow count  $N$  to the relative density of granular soils as shown in Fig. 4.5. Gibbs and Holz and Bazaraa (24) showed this same relationship with regard to overburden pressure as shown in Fig. 4.5.

Teng (24) gave a formula for the allowable bearing pressure based upon the Terzaghi and Peck work of 1948.

This formula is:

$$q_a = 720(N-3) \left( \frac{B+1}{2B} \right)^2 R_w D_B \quad (4.2)$$

where:

$q_a$  = net allowable bearing pressure (in psf) for a maximum settlement of 1 inch.

$R_w$  = correction factor for water table

= 1.0 for water table below bottom of footing  
= 0.5 for water table above bottom of footing

$N$  = penetration blows (in pcf-ft.)

$B$  = width of footing (in ft.)

$D_B$  = depth factor =  $1 + \frac{D}{B}$

#### 4.2.2 VANE SHEAR TEST (10, 13) (ASTM Standard D 2573-72(1978))

The Vane Shear Test is a quick test, used either in the laboratory or in the field, to determine the undrained shear strength of cohesive soil  $C_u$  ( $\phi$  = zero concept).

From experience it has been found that the Vane Test can be used for a reliable in-situ test for the shear strength of soft-sensitive clays occurring at depths beyond 10 meters. The Vane Test should be regarded as a method to be used under the following conditions:

1. where the clay is deep, normally consolidated and sensitive,
2. where only the undrained shear strength is required,

It is necessary that the soil mass should be in a saturated condition if the Vane Test is to be applied. The Vane Test cannot be applied for partially saturated soils for which the angle of shearing resistance is not zero.

Fig. 4.6 shows the Vane Shear tester (13). It consists of four thin equal sized steel plates, called vanes, welded orthogonally to a steel torque rod. The vanes are inserted into an undisturbed soil in-situ and gradually rotated at a uniform speed of 6.0 degrees per minute about the axis of the shaft called the vane axis thus creating a torque. The surface resisting the turning is the cylindrical surface of the soil and the two end faces of the cylinder. At failure the resisting moment of the cylinder of soil of height  $h$  and diameter  $d$  is equal to the turning moment applied at the torsion head.

The undrained cohesion of the soil can be calculated as follows:

The maximum torque  $T$  applied at the head of the torque rod to cause failure should be the sum of the resisting moment of the shear force along the side surface of the soil cylinder,  $M_s$ , and the resisting moment of the shear force at the ends,  $M_e$ , or

$$T = M_s + M_e \quad (4.3)$$

The assumed distribution of shear stress on the side surface of the soil cylinder and on the two ends (zero at the center and at the periphery) is shown in Fig. 4.7. Thus,

$$M_s = (\pi dh) \left( \frac{d}{2} \right) C_u \quad (4.4)$$

$$M_e = 2 \left( \pi \frac{d^2}{4} \right) \left( \frac{2}{3} \frac{d}{2} \frac{C_u}{2} \right) \quad (4.5)$$

where  $d$  = diameter and  $h$  = height of the shear vane.

Substituting Eqs. (4.4) and (4.5) into Eq. 4.3, we get

$$T = \left( \pi \frac{d^2 h}{2} + \pi \frac{d^3}{12} \right) C_u ; C_u = \frac{T}{\left( \pi \frac{d^2 h}{2} + \pi \frac{d^3}{12} \right)} \quad (4.6)$$

However, if only one end of the vane, i.e., the bottom, is involved in shearing the clay,

$$M_e = \pi \cdot C_u \cdot \frac{d^3}{24} \quad \text{and}$$

$$C_u = \frac{T}{\left(\pi \frac{d^2 h}{2}\right) \left(1 + \frac{d}{12}\right)} \quad (4.7)$$

Vane shear tests can be conducted in the laboratory and in the field during soil explorations. The laboratory shear vane has dimensions of about 0.5 in. in diameter and 1.0 in. in height. Field shear vanes with the following dimensions are used by the U.S. Bureau of Reclamation:

$d = 2.0$  in. (50.8 mm.),  $h = 4$  in. (101.6 mm.),  
 $h/d = 2$ .

The vane may be pushed down from the surface, measurements being made at regular intervals. The shaft on which the vane is mounted is enclosed within a sleeve, to prevent adhesion to the soil. In suitable soils, tests have been made in this way at depths exceeding 60 m.

#### 4.2.3 THE 'DUTCH' CONE PENETROMETER (14) (ASTM Standard D 1558-71(1977))

The estimation of the static shear strength of the soil by means of a dynamic test is inherently unsatisfactory, largely because the pore stresses differ in the two conditions, and the standard penetration test results cannot provide more than a rough guide to the soil properties. More reliable results are obtained from static penetration tests, of which the most commonly used is the 'Dutch' cone penetrometer (14). This device has been used

extensively in Holland and Belgium, mainly in fine sands and silts.

The penetrometer (14) is cone shaped, with a maximum area of 1000 sq. mm. The cone is attached to a rod, which is protected by an outer sleeve. The thrust needed to drive the cone and the sleeve into the ground may be measured independently, so that the end bearing resistance and the side friction may be separately determined.

The penetrometer, as shown in Fig. 4.8, was developed for the design of piles, but it has also been used successfully to estimate the bearing capacity and settlement of foundations on non-cohesive soils.

The soil specimen is penetrated at the rate of 0.5 in. per second for a distance of not less than 3 in. The penetrometer has interchangeable needles whose sizes are shown in Table 4.2 (14).

The penetration resistance of the soil is the product of the penetrometer reading and the reciprocal of the end area of the needle and is expressed in pounds-force per sq. in..

#### 4.2.4 PRESSUREMETER (15)

The Fugro Full Displacement Pressuremeter (FDPM) (15)

has been developed to make it easier to obtain off-shore in-situ measurements of stress-strain properties. The prototype FDPM (Fig. 4.9) can cover a reasonably wide range of strain and the equipment is in principle easier to deploy and operate by remote control in conventional off-shore drilling operations.

The FDPM test is performed as part of the cone penetration test. When the center of the pressuremeter membrane reaches the test depth, the cone penetration is halted and then resumed when the pressuremeter membrane is deflated. Fig. 4.10 (15) shows the set up for prototype FDPM testing.

Advantages of the FDPM are:

1. the ease of operation
2. measurement of stress-strain properties at a depth known precisely in relation to the cone resistance profile. It reduces scatter and improves correlation of soil strength and stiffness with cone resistance.

The overall length of the membrane is 450 mm. The outer diameter is 43.7 mm. (the same as that of the 15 sq. cm. cone). Length to diameter ratio is 10.3. Above the pressuremeter is a module which amplifies the pressuremeter signals. It measures inflation pressure and, at three locations 120 degrees apart, the circumferential strain. Inflation is achieved with nitrogen gas.

There are three other types of pressuremeters.

The first was developed by L. Menard. The pressuremeter lowered into a predrilled hole, measurements of pressure and volumetric strain are made. Results are highly sensitive to soil disturbance from drilling and stress relief at the bore hole wall, neither of which can be measured.

The second type, the Self Boring Pressuremeter was developed to minimise soil disturbance. Measurements are made of total pressure, pore pressure, and circumferential strain at three positions at the midheight of the expanding length.

The third type, the Push In Penetrometer (PIP) was developed for off-shore use. Inflation of the membrane is by oil and the pressure and volumetric strain are measured.

#### 4.2.5 DIRECT SHEAR TEST (1, 13, 14) (ASTM Standard D 3080-72(1979))

The Direct Shear Test is the oldest and simplest shear test arrangement (Fig. 4.11). A schematic diagram of the apparatus is shown in Fig. 4.12. The relatively thin thickness of sample permits quick drainage and quick dissipation of pore pressure developed during the test.



The shear box containing the soil sample is generally kept inside a container that can be filled with water to saturate the sample. A shearing force is applied to the sample such that the sample shears at a constant rate of strain. The shearing resistance is measured on a proving ring and the maximum value is the shear strength of the soil. This shear strength may be found with the sample subjected to varying compressive loads and a graph of shear stress against compressive stress is plotted as in Fig. 4.13.

#### Controlled-stress and Controlled-strain Tests (6, 14)

Fig. 4.14 (6) illustrates the difference between these two types of tests, as applied to direct box shear tests. In the first type(a, Fig. 4.14) the load  $P_t$  which induces shear is gradually increased until complete failure occurs. The shearing displacements are measured by means of the dial gage a as a function of the increasing load  $P_t$ . In the second type(b, Fig. 4.14), the shearing displacements are induced and controlled in such a manner that they occur at a constant fixed rate. The dial gage a registers the desired constant rate of displacement. The shearing resistance offered to this displacement by the soil specimen is measured by the proving ring f.

However, the test has the following inherent



disadvantages:

1. the stress conditions across the soil sample are very complex. The distribution of normal stresses over the potential surface of sliding is not uniform. The stress is more at the center than at the edges. Due to this there is progressive failure of the specimen, i.e. the entire strength of the soil is not mobilized simultaneously.
2. as the test progresses, the area under shear gradually decreases. The corrected area at failure should be used in determining the value of  $c$  and  $\phi$ .
3. unlike the triaxial test, there is no control on the drainage of the soil.
4. the plane of shear failure is predetermined, which may not be the weakest one.
5. there is effect of lateral restraint by the side walls of the shear box.

#### 4.2.6 THE TRIAXIAL COMPRESSION TEST (1, 16, 25) (ASTM Standard D 2850-82)

A soil sample may be tested in the general stress state  $(\sigma_1 > \sigma_2 > \sigma_3)$  , while at the same time, the deformations and volume changes are also measured. In order to evaluate a subgrade soil by means of this strength test, it is necessary to simulate, in a laboratory specimen, stress conditions existing in the loaded soil mass. This test is the most common test for the evaluation of the stress-strain characteristics of the soil.

A schematic illustration of the Triaxial Compression Cell is shown in Fig. 4.15 (6).

In this stress test, a cylindrical specimen about 1.5 in. in diameter and 3 in. in length is first encased in a thin rubber membrane and subjected to fluid pressure around the cylindrical surface which equally stresses all surfaces of the specimen, usually by water, sometimes by air. Then an axial load is applied and its magnitude is increased. Although only compressive stresses are applied, the specimen generally fails by shearing, hence the test is generally referred to as the Triaxial Shear Test. In some cases, failure occurs by bulging. In the typical triaxial test, usually the cylindrical soil samples are

examined in an axially symmetrically stressed state ( $\sigma_1 \gg \sigma_2 = \sigma_3$ )  
The soil is failed by increasing the axial stress while holding the confining stress constant. Axial force is applied to the loaded piston either by means of dead weights (controlled stress test) or by a geared or hydraulic loading press (controlled strain test). Selection of the rate of loading of the specimen depends upon design conditions, i.e. whether the field loading conditions will be static, dynamic, or some combination.

The applied axial load produces normal vertical stresses on each horizontal face of the specimen, while the lateral pressure produces normal horizontal stress on any two vertical planes at right angles to each other. These vertical and horizontal stresses fulfill the requirements of principal stresses, since there are no components of applied loads to produce shearing stresses in the horizontal plane or either of the vertical planes. The vertical stress is the maximum principal stress. The horizontal stress on the vertical plane is the minimum principal stress, and that on the vertical plane normal to the minimum principal plane is the intermediate principal stress. The minimum and intermediate principal stresses are equal in this case. However, since the intermediate principal stress does not influence the failure of the

material, according to the Mohr Theory, it need not be considered further.

The inherent stability of a soil is represented by the general Coulomb equation (2):

$$S = c + \sigma \tan \phi \quad (4.8)$$

The use of the Coulomb equation to represent internal stability is predicted on the assumption that the internal resistance of materials is a function of the shearing resistance due to internal friction. The subject of shearing resistance of soils is extremely complex, particularly from the standpoint of design of pavements. If full drainage of the sample is permitted during the test, the water can move into and out of the pores. Soft and saturated clays can behave as if they possess no internal friction ( $\phi=0$ ).

Therefore, the Coulomb equation becomes:

$$S = c \quad (4.9)$$

The shearing resistance of cohesionless materials can be written as:

$$S = \sigma \tan \phi \quad (4.10)$$

Fig. 4.16 shows the shear stress vs. normal compressive stress relationships for the three types of soils;  $c = 0$  soils,  $\phi = 0$  soils, and  $c-\phi$  soils.

There are a number of ways in which the triaxial test

can be performed. For example, triaxial extension tests can be run by maintaining  $(\sigma_1)_1$  constant and increasing the confining pressure  $(\sigma_3)_1$ . Also, triaxial tests can be run under at rest earth pressure conditions by increasing  $(\sigma_1)_1$  and simultaneously such that no lateral deformation of the sample takes place.

When one cylindrical sample has been loaded to failure, a Mohr Circle may be drawn having a diameter equal to  $(\sigma_1)_1 - (\sigma_3)_1$ , or the difference between the vertical and horizontal failure stresses. There is one point on this circle which represents the combination of normal and shearing stress at which the soil failed. This point lies on the Mohr Envelope. However, unless it is definitely known that the soil is completely cohesionless, in which case the Mohr Envelope passes through the origin of the applied stresses, there is no clue as to the location of the failure point. Therefore it is necessary to conduct another test on a duplicate (or the same) sample, a different lateral pressure being applied in this test. The applied stresses at failure in this second test may be designated  $(\sigma_1)_2$  and  $(\sigma_3)_2$ , and a second Mohr Circle may be drawn with the diameter  $(\sigma_1)_2 - (\sigma_3)_2$ . Since  $(\sigma_3)_2$  is different from  $(\sigma_3)_1$ , then  $(\sigma_1)_1$  and  $(\sigma_1)_2$  will also be different and the second circle will not coincide with the first. Again

there is one point on the second circle which represents the failure stresses and lies on the Mohr Envelope. Likewise, a third test can be conducted with another confining pressure to arrive at another Mohr circle with stresses  $(\sigma_1)_3$  and  $(\sigma_3)_3$ , with a point on it that represents the stresses at which the soil failed. These failure points can be located by drawing a common tangent to the circles. This tangent is the Mohr Envelope of the soil. It is also the graph of the Coulomb equation for shearing strength of the soil as shown in Fig. 4.17.

The intercept of the tangent line on the vertical axis through the origin of applied stresses is the cohesion of the soil, and the angle that the tangent makes with the horizontal is the friction angle of the soil. Also, the intercept of the tangent line on the horizontal axis is the origin of total stresses, and the distance between the two origins represents the initial stress in the material.

The purpose of the Triaxial Compression Test of soils is to provide basic data on the following (1):

1. The ultimate laterally confined compressive strength of the soil,
2. The angle of internal friction,
3. The cohesion,

4. The shear strength of the soil,
5. The Modulus of Elasticity, and
6. The pore water pressure.

The data obtained from the Triaxial Test are used for:

1. making estimates of the probable bearing capacity of the soil,
2. performing stability calculations of earthworks, earth retaining structures, and foundations,
3. analysing stress-strain relationships of loaded soils.

The advantage of the triaxial compression test is that this test makes it possible to investigate the change in the shear strength of a soil for different ratios of major (axial) and minor (lateral) principal stresses, similar to conditions as they exist in the field. However, the outstanding advantages of the triaxial test are the control of drainage conditions and the possibility of the measurement of pore pressure. No other strength test combining these two features have been developed to a stage of practical utility. As a result, the triaxial apparatus has been used in most basic research work on shear strength and pore pressure characteristics i.e. the basic understanding of the soil properties.

It has been experimentally observed that the values of  $c$  and  $\phi$  remain almost constant over a considerable



range of strain. This fact is used to advantage when a limited amount of soil is available for testing or where the samples are variable. The MULTISTAGE TRIAXIAL (MST) tests have been developed to reduce the number of samples, and hence the time and effort required in conventional triaxial methods.

#### 4.2.6.1 Principle Of The Triaxial Compression Test (2)

An analysis of the triaxial stresses is best made by the use of Mohr's circle of stresses.

The principle of the triaxial test is illustrated in Fig. 4.18 (25). A cylindrical specimen of soil which is enclosed in a thin rubber membrane is placed in the cell. The specimen is first subjected to a constant all-round hydrostatic pressure  $p_c (= \sigma_d)$ . Water is allowed to escape through a porous disk inserted into the base of the cell, thus permitting the dissipation of the neutral stresses. In this initial state of stress, called isotropic compression, the Mohr circle reduces to a point. The axial stress is then increased by some value  $p (= \sigma_3)$ . In the conventional test, it is necessary to add the confining pressure  $p_c$  to the deviator pressure  $p$  to determine the total unit load at failure.

Thus:

$$p_c = \sigma_d = \frac{P(1-\delta)}{A} \quad (4.11)$$



where

$p_c = \sigma_d$  = deviator stress = applied stress

$P$  = applied deviator load

$A$  = original cross-sectional area

$\delta$  = unit strain

The altered state of stress is defined as:

$$\sigma_1 = p_c + p = \sigma_d + \sigma_3 ; \sigma_2 = \sigma_3 = p_c = \sigma_d$$

The deviator stress,  $p_c$ , is then gradually increased, while the confining lateral stress,  $p$ , is held constant, until the specimen fails in shear. At the ultimate stage the corresponding Mohr circle just touches the Coulomb line. By performing several tests at different initial confining pressures, a series of Mohr circles is obtained.

Fig. 4.19a is the physical representation of the stressed sample, and Fig. 4.19b is the corresponding Mohr's circle representation. The normal stresses at a point is a function of the orientation of the plane chosen to define the stress. Also, when using Mohr's circles to analyse stresses in soils, normal stress is considered positive when compressive.

Any point A on the circle of Fig. 4.19b represents the stress on a plane whose normal is oriented at an angle  $\theta$  with the direction of the major principal stresses. Thus the normal stress on the plane is:

$$\sigma_\theta = \sigma_1 \cos^2 \theta + \sigma_3 \sin^2 \theta = (\sigma_1 + \sigma_3) / 2 + (\sigma_1 - \sigma_3) / 2 \cdot \cos 2\theta$$

The shear stress on the plane located by the angle is:

$$\tau_{\theta} = (\sigma_1 - \sigma_3) \sin \theta \cos \theta = (\sigma_1 - \sigma_3) / 2 \cdot \sin 2\theta$$

When many Mohr's circles are plotted to represent many states of stress for a given soil specimen on a single diagram, it becomes difficult to follow the diagram. An alternative method for plotting the state of stress is to plot p and q. p is the stress represented by the distance to the center of the Mohr's circle from the origin and q is the stress represented by the radius of the Mohr circle. Thus, p and q are computed as follows:

q is +ve if  $\sigma_1$  is inclined at an angle  $\leq \pm 45^\circ$  to the vertical  
 q is -ve if  $\sigma_1$  is inclined at an angle  $< \pm 45^\circ$  to the horz.

For the stress point representation, the principal stresses act on vertical and horizontal planes. The equations simplify to:

$$p = (\sigma_v + \sigma_h) / 2 \quad q = (\sigma_v - \sigma_h) / 2$$

A series of values of p and q is plotted representing the successive states of stress that exist in a specimen as the specimen is loaded. Then, a series of stress points are plotted. A line is drawn connecting these points using p and q. Refer Fig. 4.20.  $K_f$  line drawn on Fig. 4.20 is defined as  $\sigma_h / \sigma_v$  at failure and is called the coefficient of lateral stress at failure.

There is no page 55 in the original.

The failure of a soil specimen used in the triaxial compression test may occur in a number of different ways. The stresses in the specimen are distributed quite uniformly around the cylindrical axis. If the specimen is uniform in strength throughout, failure will occur on a very large number of closely spaced planes making an angle  $\theta'$  with the horizontal. A failure of this kind is evidenced by a uniform bulging of the sample. Another type of failure is when the failure occurs along a single plane. Many specimens fail by a combination of the above two failure modes.

#### 4.2.6.2 Methods Of Triaxial Testing (1)

Triaxial tests can be made on either remolded or undisturbed samples. If remolded samples are to be tested, a series of compaction tests should first be made to determine the optimum moisture content and maximum density of the soil. Samples can then be molded to the required density and moisture conditions and saturated either by soaking or by vacuum saturation techniques.

Care should be exercised during the compaction procedure to make certain that the sample is uniform throughout its height, with little or no variation in its density.

This is best accomplished by a combination of impact and static compaction procedure.

Triaxial tests can be performed in any number of ways, depending upon the data desired. Quick tests are ones in which the vertical load is applied rapidly with no drainage of the sample permitted during the test. For this test, the load is applied at the rate of about 0.05 inch per minute. Quick drained tests are ones in which the samples are permitted to drain during the application of the confining pressure, but no drainage is permitted during the axial loading which is applied in a rapid manner. Slow drained tests are ones in which the sample is permitted to drain during the testing period, but, in addition, the load is applied in a slow manner permitting the samples to consolidate under each increment of load.

For the design of pavements, the quick undrained test is recommended. This is because loads applied to a pavement in service are transient, and it is doubtful whether any drainage takes place during the loading cycle. In some instances, it may be desirable to consolidate the sample before application of the load to simulate consolidation of the subgrade under the pavement. To accomplish this, the specimen is encased in a rubber membrane, and care is taken to make certain that the membrane is in

intimate contact around the testing heads. All drainage valves should be closed.

#### 4.2.6.3 Stress Condition in Specimen During Triaxial Test

Fig. 4.21 (25) shows the effective stresses acting on the soil specimen during the triaxial testing. The minor principal stress and the intermediate principal stress are equal. The effective minor principal stress is equal to the cell pressure minus the pore pressure.

The stress components on the failure plane MN are  $\sigma'$  and  $\tau$  and the failure plane is inclined at an angle  $\theta'$  to the major principal plane. JF is the failure envelope to the Mohr circle corresponding to any failure point F. Since  $\angle JFC = 90^\circ$  and the failure envelope cuts the abscissa at an angle  $\phi'$ , the angle  $\theta'$  of the failure plane is given by:  $\theta' = \frac{1}{2} \angle FCA = \frac{1}{2} (90^\circ + \phi') = 45^\circ + \frac{\phi'}{2}$

The principal stress relationship at failure can be deduced as follows:

$$FC = \frac{1}{2} (\sigma_1' - \sigma_3') \quad ; \quad OC = \frac{1}{2} (\sigma_1' + \sigma_3') \quad ; \quad OK = c' \cot \phi'$$

$$\sin \phi' = \frac{FC}{KC} = \frac{FC}{KO + OC} = \frac{\frac{1}{2} (\sigma_1' - \sigma_3')}{c' \cot \phi' + \frac{1}{2} (\sigma_1' + \sigma_3')} = \frac{(\sigma_1' - \sigma_3')}{2c' \cot \phi' + (\sigma_1' + \sigma_3')}$$

$$\therefore (\sigma_1' - \sigma_3') = 2c' \cos \phi' + (\sigma_1' + \sigma_3') \sin \phi'$$

$$\therefore \sigma_1' (1 - \sin \phi') = \sigma_3' (1 + \sin \phi') + 2c' \cos \phi'$$

$$\therefore \sigma_1' = \sigma_3' \left( \frac{1 + \sin \phi'}{1 - \sin \phi'} \right) + 2c' \left( \frac{\cos \phi'}{1 - \sin \phi'} \right)$$

$$\text{or } \sigma_1' = \sigma_3' \tan^2\left(45^\circ + \frac{\phi'}{2}\right) + 2c' \tan\left(45^\circ + \frac{\phi'}{2}\right) \quad (4.12)$$

$$\text{or } \sigma_1' = \sigma_3' \tan^2 \theta' + 2c' \tan \theta' = \sigma_3' N_{\phi'} + 2c' \sqrt{N_{\phi'}} \quad (4.13)$$

$$\text{where } N_{\phi'} = \tan^2 \theta' = \tan^2\left(45^\circ + \frac{\phi'}{2}\right)$$

Eqs. 4.12 and 4.13 give the principal stress relationship. When the soil is in the state defined by the eqs. 4.12 or 4.13, it is said to be in plastic equilibrium. In terms of total stress, eqn. 4.13 is written as:

$$\begin{aligned} \sigma_1 &= \sigma_3 \tan^2 \theta + 2c \tan \theta \\ &= \sigma_3 N_{\phi} + 2c \sqrt{N_{\phi}} \\ \theta &= 45^\circ + \frac{\phi}{2} \\ N_{\phi} &= \tan^2 \theta = \tan^2\left(45^\circ + \frac{\phi}{2}\right) \end{aligned}$$

In eqn. 4.12,  $\sigma_1'$  and  $\sigma_3'$  are known, and the two unknowns are  $\phi'$  and  $c'$ . Hence two sets of observations are required to determine these two unknown parameters. In practice, a number of sets of  $(\sigma_1', \sigma_3')$  at failure are observed, and the Mohr circles are plotted for each set of values. A curve drawn tangential to these circles gives the failure envelope.

#### 4.2.6.4 Application of the Triaxial test to the principal soil types (1)

The application of the triaxial test to the principal soil types may be considered under the following classifications:

1. undrained test on saturated cohesive soils,
2. undrained test on partly saturated cohesive soils,
3. consolidated-undrained test on saturated soils,
4. drained test.

#### 4.2.6.4.1. Undrained Test on Saturated Cohesive Soils

This test is carried out on undisturbed samples of clay, silt or peat to determine the strength of natural ground. It is also carried out on remolded samples of clay to measure its sensitivity (1).

The results of this test are illustrated in Fig. 4.22. (13).

For a fully saturated soil, the pore pressure parameter  $B$  equals unity. In an undrained test ( $\Delta\sigma_3$  equals zero), on saturated clays, both the major principal effective stress  $\sigma_1' (= \sigma_1 - u)$  and the minor principal effective stress  $\sigma_3' (= \sigma_3 - u)$  are independent of the magnitude of the cell pressure applied. Thus, only one effective stress circle can be obtained from these tests and the shape of the failure envelope in terms of effective stress cannot be determined. Pore pressure measurements are not usually made during undrained tests on saturated samples.

The shear strength of the soil is used in stability analysis in terms of total stress, which, for this type of



soil, is known as the  $\phi=0$  analysis. The failure stress is taken to be the maximum deviator stress which the sample can withstand.

#### 4.2.6.4.2. Undrained Test on partly saturated cohesive soils (1, 13)

The most common application of this test is to samples of earth-fill material which are compacted in the laboratory under specified conditions of water content and density. It is also applied to undisturbed samples of strata which are not fully saturated (residual soils), and samples cut from existing rolled fills.

As the cell pressure is increased, the deviator stress at failure also increases, though this increase in deviator stress becomes progressively smaller as the air in the soil voids is compressed and dissolved. The increase in the deviator stress later ceases when the large stresses cause full saturation. Due to this reason, the failure envelope in terms of total stresses is non-linear, as shown in Fig. 4.23. The values of  $c$  and  $\phi$  can, therefore, be quoted only for a certain pressure range. However, if the pore pressure is measured during the test, the failure envelope can be expressed in terms of effective stress, and is found to approximate very closely to a straight line over a wide range of stress. Apparent

departures from linearity are usually found to be due to small differences in water contents between the different samples used to define the envelope.

#### 4.2.6.4.3. Consolidated-Undrained test on saturated soils

The consolidated-undrained test is carried out on undisturbed samples of clay, silt and peat, on remolded samples of clay and silt, and on redeposited samples of cohesionless soil such as sand and gravel (1, 13).

In the standard test, the results of which are depicted in Fig. 4.24 (13), the sample is allowed to consolidate under a pressure of known magnitude, the three principal stresses thus being equal. Then the sample is sheared under undrained conditions with different cell pressure by increasing the axial load, the deviator stress being independent of the cell pressure. It is observed that the apparent cohesion increases linearly with the increasing effective consolidation pressure; for normally consolidated soil, the graph of undrained strength ( $C_u$ ) and consolidation pressure ( $\bar{p}$ ) passes through the origin. If the clay is preconsolidated (over consolidated), the curve is non-linear upto the preconsolidation pressure; however, at higher consolidation pressure, the soil behaves as a normally consolidated soil and a linear rela-

tionship is obtained.

However, if the pore pressure is measured during the undrained stage of the test, the results can be expressed in terms of effective parameters  $c'$  and  $\phi'$ . For normally consolidated samples, the effective stress envelope is a straight line with  $c'$  equal to zero.

Reconsolidation in the laboratory after the disturbance which is associated even with the most careful sampling leads to a slightly higher void ratio than would occur in nature. The most marked effect of over-consolidation is, however, on the value of pore pressure parameter A, which, with increasing over-consolidation ratio, drops from a value typically about 1 at failure to values in the negative range. These low A-values are, in turn, largely responsible for the high undrained strength values resulting from over-consolidation.

For these reasons, the results of consolidated-undrained tests, expressed in terms of total stress, can be applied in practice only to a very limited extent.

#### 4.2.6.4.4 Drained Test (1, 13)

Drained tests are carried out on soil samples of all types either undisturbed, remolded, compacted, or redeposited. The samples may be either fully or partly satu-

rated. These tests are carried out to obtain directly the shear strength parameters relevant to the conditions of long-term stability, when the pore pressure have decreased (or increased) to their equilibrium values. Cohesionless materials such as sand, gravel, and rock-fill are often tested dry as it simplifies laboratory procedure. This may, however, lead to a slight over-estimate of the value of  $\phi$  in some cases.

Fig. 4.25 (13) documents the effective stress failure envelope obtained from drained tests in sand.

In the standard test (1), the specimen is first consolidated under an equal all-round cell pressure, and the sample is then sheared by increasing the axial load at a sufficiently slow rate to prevent any buildup of excess pore pressure. The minor principal stress at failure  $\sigma_3'$  is thus equal to the consolidation pressure; the major principal stress  $\sigma_1'$  is the axial stress. Since the pore pressure is zero, the effective stresses are equal to the applied stresses, and the strength envelope in terms of effective stresses is obtained directly from the stress circle at failure. The values of the effective parameters  $c'$  and  $\phi'$  obtained from drained tests are often denoted  $c_d$  and  $\phi_d$  respectively.

The drained test also provides information on the

volume changes which accompany the application of the all-round pressure and the deviator stress, and on the stress-strain characteristics of the soil.

4.2.7 UNCONFINED COMPRESSION TEST (13, 25)  
(ASTM Standard D 2166-66(1977))

A special form of the triaxial test often used in soil engineering is the unconfined compression test- a triaxial compression test in which the lateral stresses are zero. Such a test can be easily and rapidly performed and can provide valuable information in the comparison of one soil with another. The unconfined compression test is only possible where the soil possesses significant amounts of cohesion so that a sample can stand unsupported.

Coulomb's equation of shear strength (25) is:

$$S = c + \sigma \tan \phi \quad (4.14)$$

where

$S$  = shear stress

$c$  = cohesion

$\sigma$  = normal stress

$\phi$  = angle of shearing resistance

For undrained tests of saturated clayey soils (  $\phi = 0$  condition),  $S = c_u$  (4.15)

where  $c_u$  = undrained cohesion

In this test, the parameter of principal concern is the maximum stress to which the sample can be subjected without failure or, in other words, the stress at which failure in the soil specimen occurs is referred to as the

unconfined compression strength.

For saturated clay specimens, the unconfined compression strength decreases with the increase of moisture content of the soil. For unsaturated soils, with the dry unit weight remaining constant, the unconfined compression strength decreases with the increase of the degree of saturation.

Some fine grained clay soils are highly plastic, and practically all their shearing strength are attributable to cohesion. In other words, the Mohr Envelope is approximately a horizontal line, the angle  $\phi = 0$ . All Mohr circles of a series representing failure of such a material will have the same diameter. In other words, the value of  $\sigma_1 - \sigma_3$  is a constant regardless of the magnitude of the minimum principal stress. Also, the Mohr Envelope is tangent to the circles at their highest points; and the cohesion is equal to the radius of the circle, or  $(\sigma_1 - \sigma_3)/2$  as in Fig. 4.26 (25).

When a cylindrical sample of clayey soil is tested in unconfined compression,  $\sigma_3 = 0$  and  $\sigma_1$  equals the vertical stress at which the sample fails. Therefore, the shearing strength of a cohesive soil without friction is equal to one-half of the unconfined compression strength of the soil.

Essentially, the test consists of gradually loading a



cylindrical soil sample at its two ends until it is destroyed by brittle or plastic failure. The vertical compression of the sample is measured throughout the loading process while the sample may deform laterally without confinement. The test is suitable for obtaining an idea of the "in-situ" strength of the individual soil strata. In addition, it is regarded as characteristic of the soil consistency. Table 4.1 shows the general relation of the consistency and the unconfined compression strength of clays.

If a clay specimen is first subjected to unconfined compression in its undisturbed, natural state, then remolded and tested again with its water content held constant, it usually exhibits much lower strength in the remolded state. This loss in strength is associated with changes in the clay structure. Remolding has a two-fold effect: it temporarily disturbs the oriented arrangement of the molecules in the adsorbed layers and destroys the stable flocculated structure of the clay formed during sedimentation. The soil will later regain a portion of the strength lost through the reorientation of the molecules (thixotropy), but the remaining loss in strength due to structural destruction is irreversible (13).

The compressive strength obtained by the unconfined



compression test is not truly representative of the in-situ strength of the soil. First of all, the unconfined compressive strength as measured in this test is greatly affected by the size of the specimen and by the test conditions, especially the rate of loading. In addition, there are always inevitable disturbances during the sampling operation. Hence, the unconfined compressive strength should primarily be regarded as an index property suitable to characterize soil consistency only.

#### 4.2.8 APPLICATION OF THE TRIAXIAL TEST TO THE SOLUTION OF ENGINEERING PROBLEMS (1)

The problems may be divided into two main classes in which:

1. the pore pressure is independent of the magnitude of the total stresses acting in the soil, and
2. the pore pressure depends on the magnitude of the stresses acting in the soil and on the time which has elapsed since their application.

##### 4.2.8.1. Analysis in which pore pressure is an independent variable (1)

- a). Long-term stability of slopes, earth fills and earth retaining structures.

The analysis is carried out in terms of effective stress using the values of  $c'$  and  $\phi'$  obtained from the

drained tests. The values of  $c'$  and  $\phi'$  may alternatively be taken from consolidated-undrained tests in which pore-pressure measurements are made. The values of the pore pressure  $u$  is obtained from a flow-net or from field measurement. The highest wet season values represent the most critical condition.

Total stress methods are sometimes applied to the analysis of existing slopes in which the pore pressure has reached its long-term equilibrium value. The undrained strength of undisturbed samples from the slope is used in the analysis.

b). Stability of slopes of sand or gravel subject to the drawdown of impounded water.

In relatively pervious soils of low compressibility the distribution of pore pressure on drawdown is controlled by the rate of drainage of pore water from the soil. This case is of practical importance where the operation of hydro-electric schemes subjects fill, normally considered as free draining, to very high rates of drawdown. The values of  $c'$  and  $\phi'$  used in the analysis are taken from drained tests or consolidated-undrained tests with the measurement of pore pressure.

4.2.8.2. Analysis in which pore pressure is a function of the stress change (1).

- a). Initial stability of the foundation of a structure or embankment on saturated clay; the initial stability of an open cut or sheet piled excavation made in clay; the initial stability against bottom-heave of a deep excavation in clay.

The analysis is carried out in terms of total stress using the value of  $\phi'$  obtained from the undrained tests on undrained samples because the stress change likely to lead to failure occurs under undrained conditions.

Care should be taken during sampling particularly in the case of sensitive soils because sampling disturbance is more marked in its effect on the undrained strength than on the values of  $c'$  and  $\phi'$ .

- b). Stability of the clay foundation on an embankment or dam where rate of construction permits partial consolidation.

The analysis is carried out in terms of effective stress using the values of  $c'$  and  $\phi'$  obtained from drained tests or consolidated-undrained tests with the measurement of pore pressure. Field measurements of pore pressure during construction is desirable to corroborate laboratory measurements. The magnitude of the initial pore pressure is controlled not only by the vertical stress due to the

weight of the embankment but also by the shear stress set up beneath it. The value of  $A$  necessary for this calculation is obtained from the consolidated-undrained test.

c). Stability of impervious rolled fill.

The analysis is carried out in terms of effective stress using the values of  $c'$  and  $\phi'$  obtained from undrained tests with measurement of pore pressure in which the major and minor principal stresses are increased simultaneously to approximate the actual stress conditions in the embankment. The rate of dissipation of pore pressure is obtained from tests in the triaxial apparatus in which the rate of decrease of pore pressure is measured at one end of the sample while drainage is permitted from the other end. Difficulties arise in reproducing field conditions in the laboratory with regard to:

i. varying moisture content:

The excess pore pressure, in certain soils, get doubled by a 1% increase in the water content.

Although  $\phi'$  remains almost unchanged by variations, the value of  $c'$  drops rapidly with an increase in water content.

ii. rolled fill materials containing stones:

The coarser fraction of the natural material (which

is omitted from tests on clay) has a significant effect on the relationship between water content and density. This difficulty applies mainly to the magnitude of the pore pressure.

- d. The stability of impervious rolled fill, and of natural slopes and cuts in clay, subject to rapid drawdown.

The analysis is performed in terms of effective stress using the values of  $c'$  and  $\phi'$  measured in consolidated-undrained tests in which full opportunity has been given for saturation to occur. In this test the sample is allowed to saturate and consolidate under the principal stress ratio obtained before drawdown, and is then subjected to the appropriate stress change under undrained conditions. The overall effect of consolidation and saturation is a drop in the value of  $c'$ , the value of  $\phi'$  remaining almost unchanged; the value of  $c'$  found to be controlled almost entirely by the water content at which the test is run.

#### 4.2.9 LIMITATIONS OF THE TRIAXIAL COMPRESSION TEST (1)

The limiting factors may be briefly summarized as:

1. influence of the value of the intermediate principal stress
2. change in principal stress directions
3. influence of end restraint
4. duration of test

1. Influence of the value of the intermediate principal stress

In the cylindrical compression test the intermediate principal stress  $\sigma_2$  is equal to the minor principal stress. In many practical problems, the value of  $\sigma_2$  will be higher than  $\sigma_3$ . This will influence both  $c'$  and  $\phi'$  and the pore pressure parameters A and B.

2. Change in principal stress directions

In the cylindrical compression test the principal planes are fixed in relation to the axis of the specimen. This restriction is unimportant in problems involving active or passive pressures in zones with a horizontal boundary, but in problems where the direction of the major principal stress changes steadily under the applied stresses this restriction limits the accuracy with which pore

pressure can be predicted.

In soils which are laminated as a result of over-consolidation or method of compaction, the values of  $c'$  and  $\phi'$  will be influenced by the inclination of the plane on which the maximum shear stress occurs.

### 3. Influence of end restraint

Friction between the ends of the specimen and the rigid end caps necessary to transfer the axial load restricts lateral deformation adjacent to these surfaces. This leads to a departure from the condition of uniform stress and strain. This affects:

i. strength characteristics:

No significant error occurs in the strength measurements, provided that the length to diameter ratio is about 2.

ii. volume change characteristics:

In the standard test, the cell pressure is generally applied first, and the decrease in diameter which accompanies the reduction in volume is resisted locally by end-restraint. As the deviator stress is applied the diameter tends to increase, and this again is opposed by end-restraint.

iii. Pore pressure characteristics:

In the undrained test non-uniformity of pore pressure is likely to result from end-restraint. Where this nonuniformity is of appreciable magnitude, it leads to a migration of pore pressure. The extent to which this readjustment occurs depends on the



permeability of the sample, its dimensions and the rate of testing.

#### 4. Duration of test

The duration of test commonly used in the triaxial apparatus and the parameters by which the results are expressed do not take into account the phenomena of creep in soils. However, in the case of over-consolidated clays, in which shear may result in a drop in pore pressure under undrained conditions, delayed failure may be the consequence of the increase in pore pressure which occurs with passage of time as equilibrium ground water conditions are reestablished.

For long-term stability problems in which the solution is based on effective stress parameters and on calculated or observed pore pressures, the drained test normally used is performed in a time varying from one-half to three days depending on soil type.

The routine undrained test on undisturbed samples is often performed in about 10 minutes.



Con- sistency	$q_u$ in tons/ ft <sup>2</sup>					
	Very Soft	Soft	Medium	Stiff	Very Stiff	Hard
$N$	<2	2-4	4-8	8-15	15-30	>30
$q_u$	<0.25	0.25-0.50	0.50-1.00	1.00-2.00	2.00-4.00	>4.00

Table 4.1 Relation of consistency of clay, number of blows  $N$  on sampling spoon, and unconfined compression strength.  
(25)

Size (area) (in. <sup>2</sup> )	1	3/4	1/2	1/3	1/5	1/10	1/20
End $\phi$ (in.)	1.124	0.976	0.796	0.651	0.505	0.357	0.252

Table 4.2 Sizes of Penetrometer needles. (24)

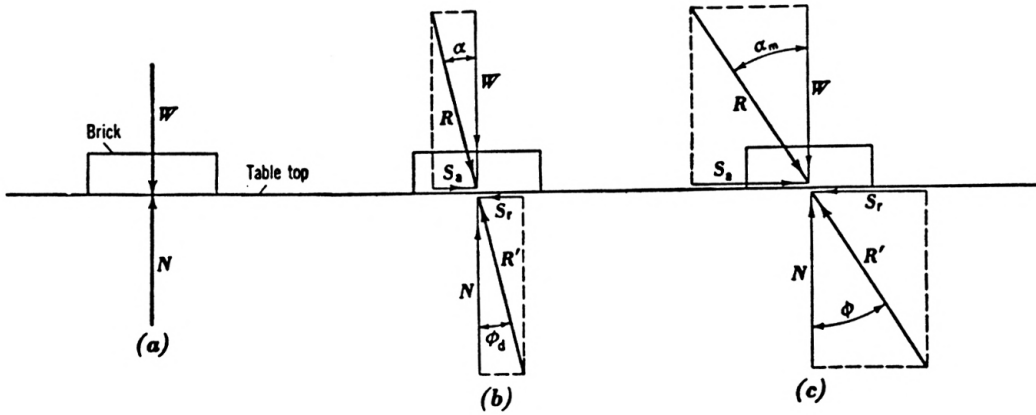


Figure 3.1 Friction on horizontal surface. (3)

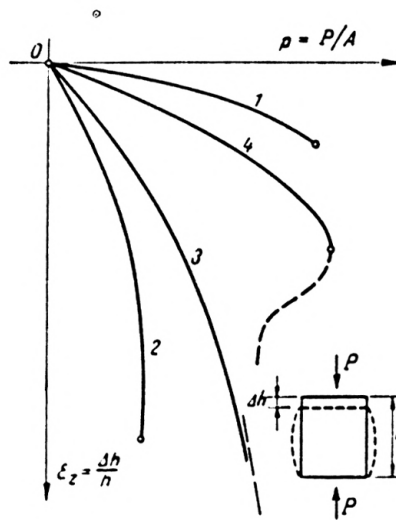
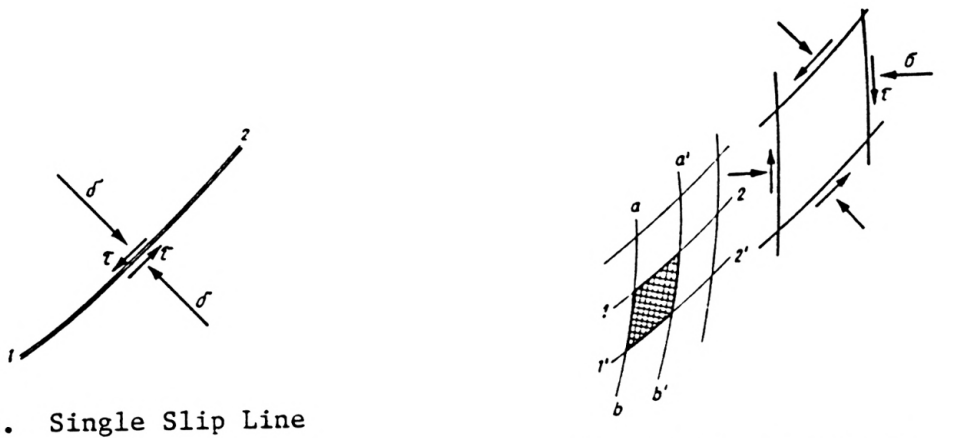


Figure 3.2 Modes of failure in soils. (5)



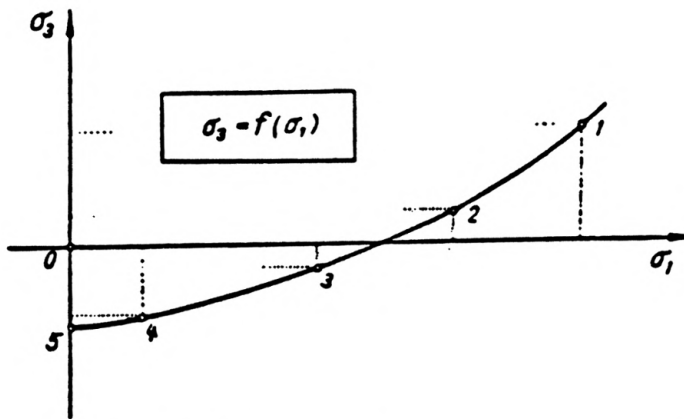
a. Single Slip Line

b. Family of Slip Lines

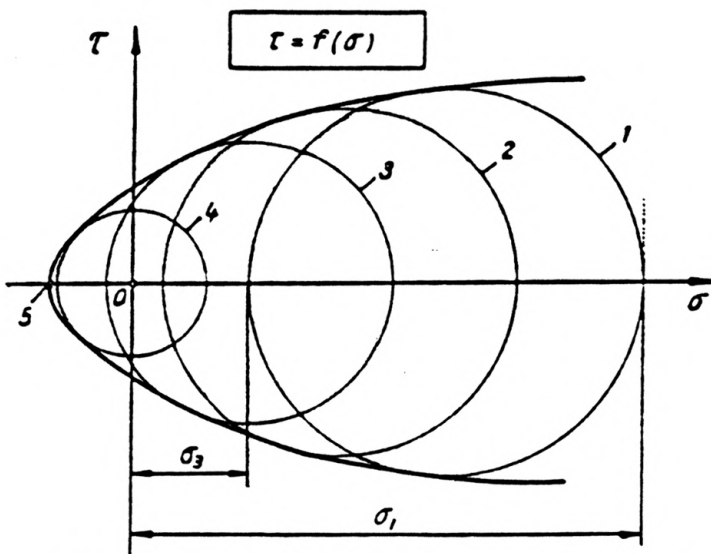
Figure 3.3 Shear Pattern. (5)



Figure 3.4 Graph of Coulomb Formula for shearing strength of soils.  
(24)



a. Relationship between major and minor principle stresses in the case of failure.



b. Envelope of Mohr's circles: 1-5 = Mohr's circles.

Figure 3.5 (5)

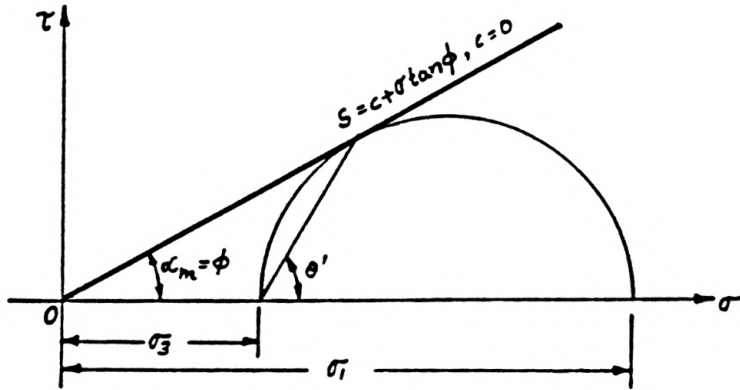


Figure 3.6 Mohr Diagram for Normal and Shearing Stresses. (24)

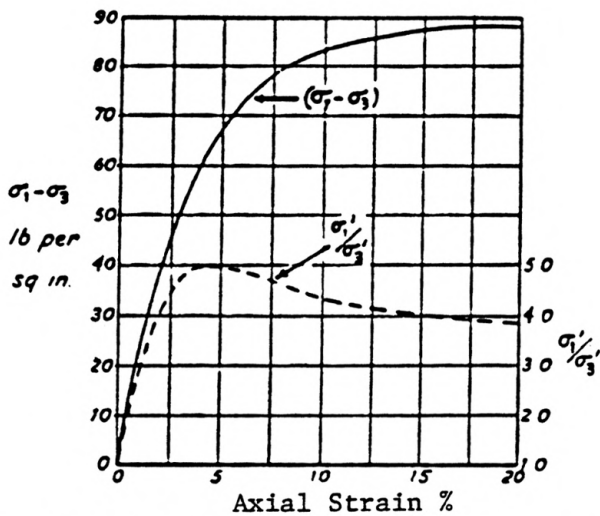


Figure 3.7 Graph of  $\sigma_1 - \sigma_3$  vs. axial strain for undrained test on compacted fill material. (1)

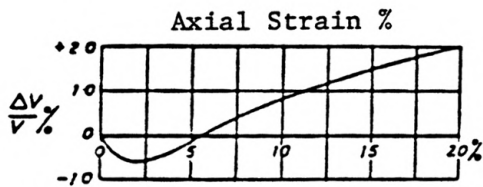


Figure 3.8 Graph of volumetric strain vs. axial strain for undrained test on a compacted fill material. (1)

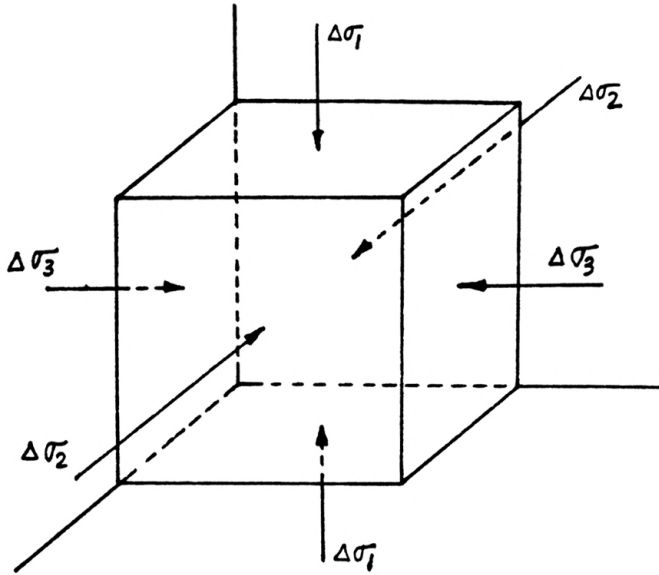


Figure 3.9 3-D loading followed by 1-D loading of soil. (1)

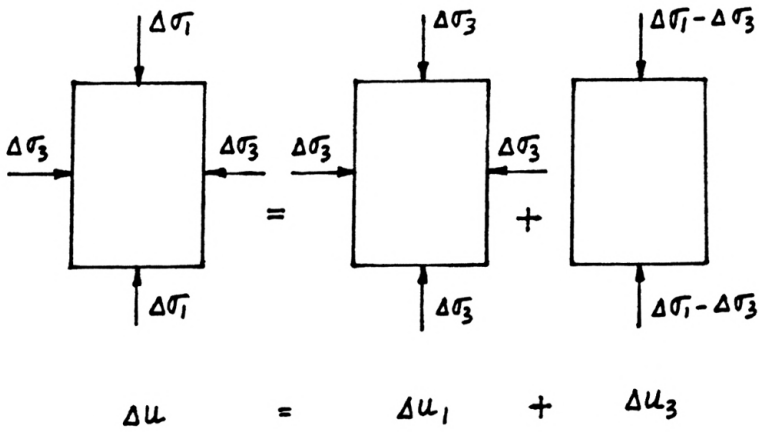


Figure 3.10 Stress change stages in Triaxial test. (24)

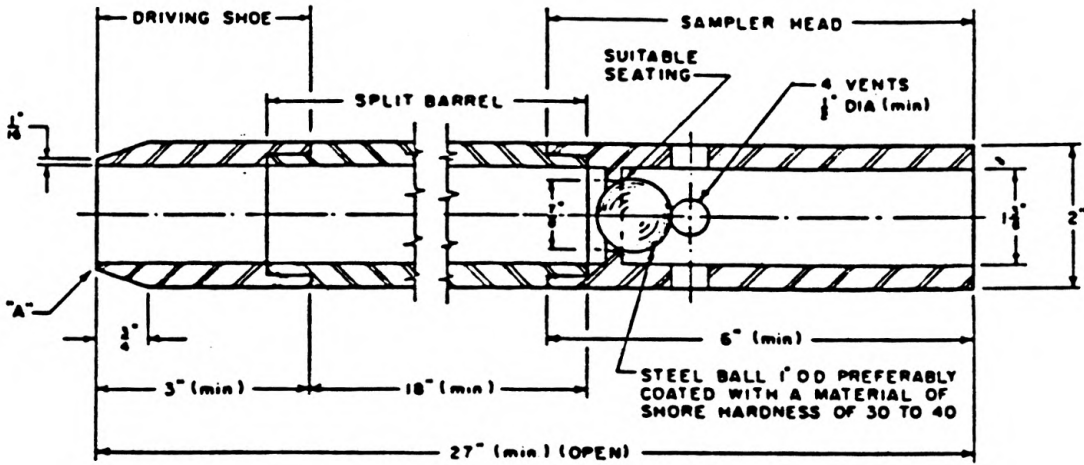


Figure 4.1 Standard Split Barrel Sampler Assembly. (25)

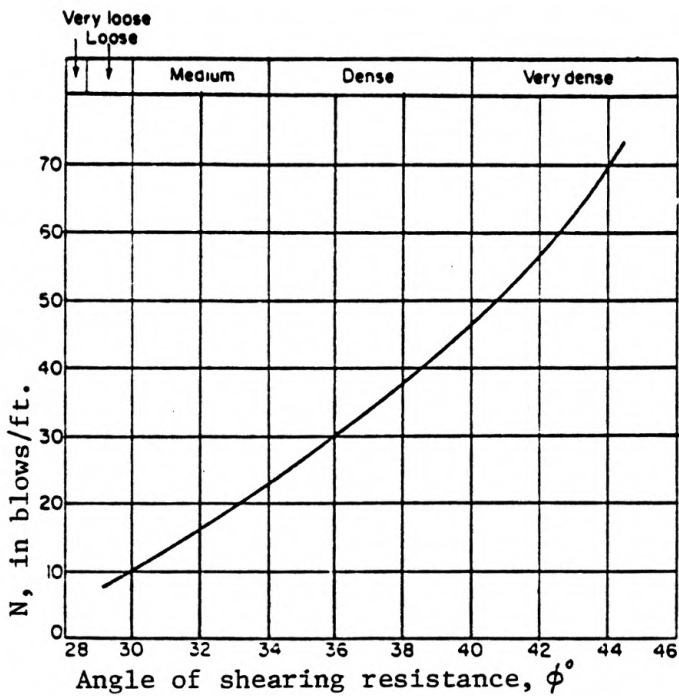


Figure 4.2 Relation between relative density,  $\phi^\circ$ , and N obtained from the Standard Penetration Test. (After Peck, Hanson, and Thornburn). (24)

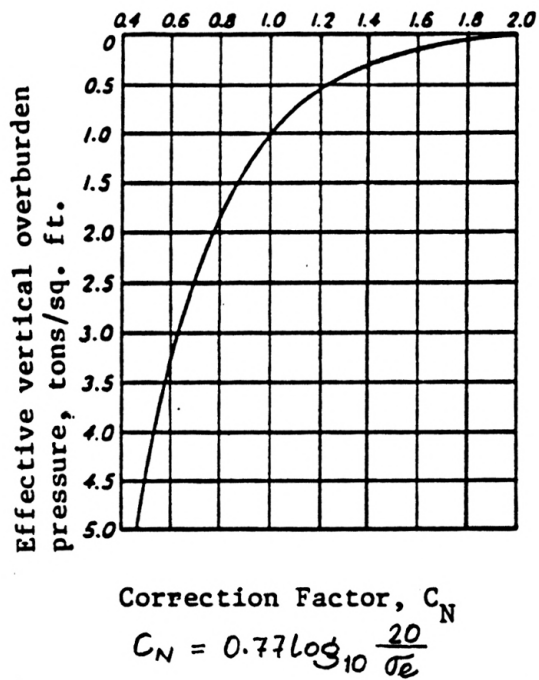


Figure 4.3 Chart for correction of N value in sand for influence of overburden pressure. (24)

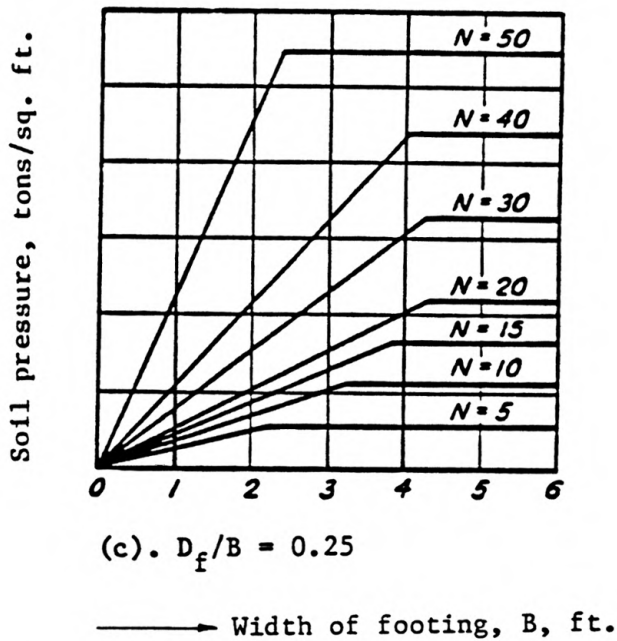
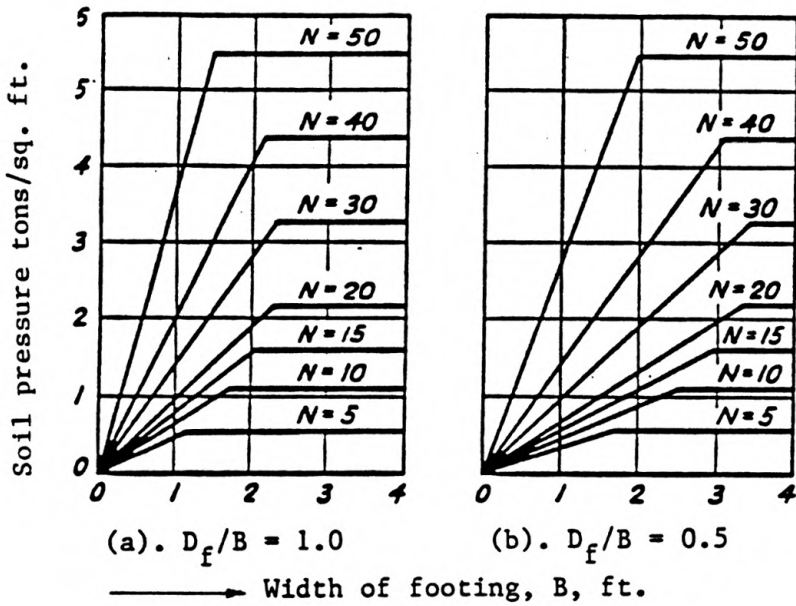


Figure 4.4 Design chart for proportioning shallow footings on sand. (24)



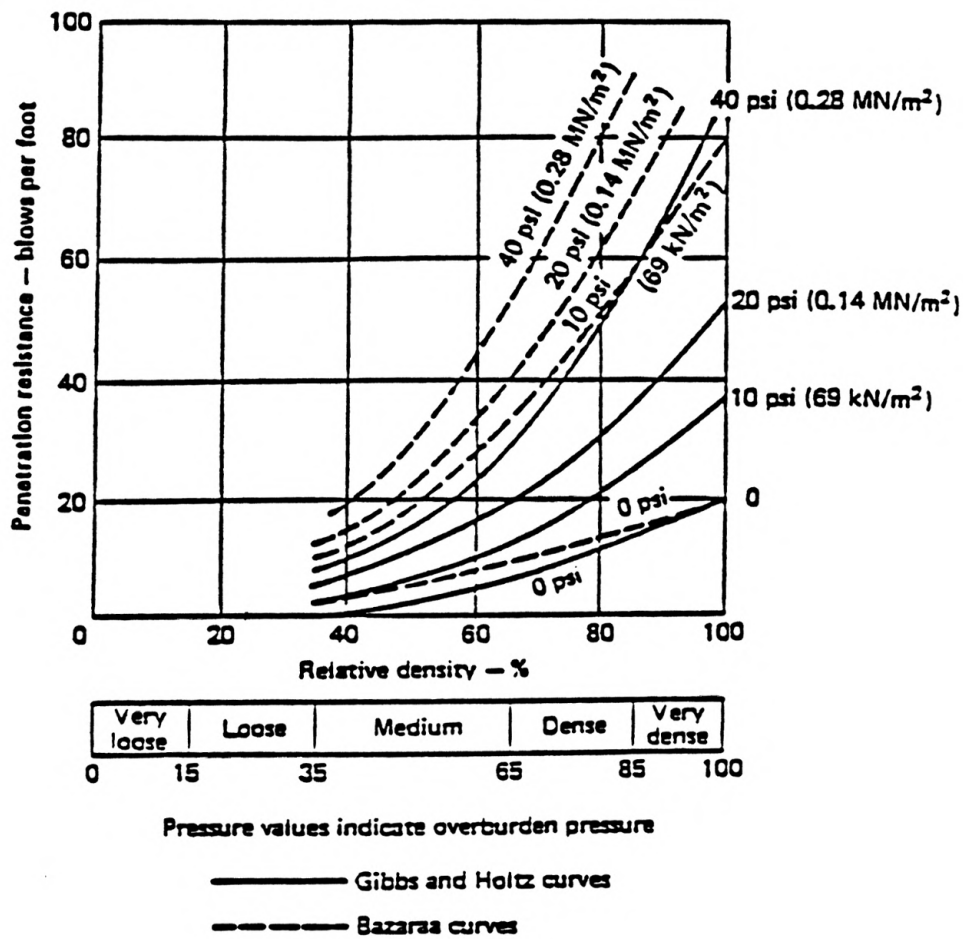
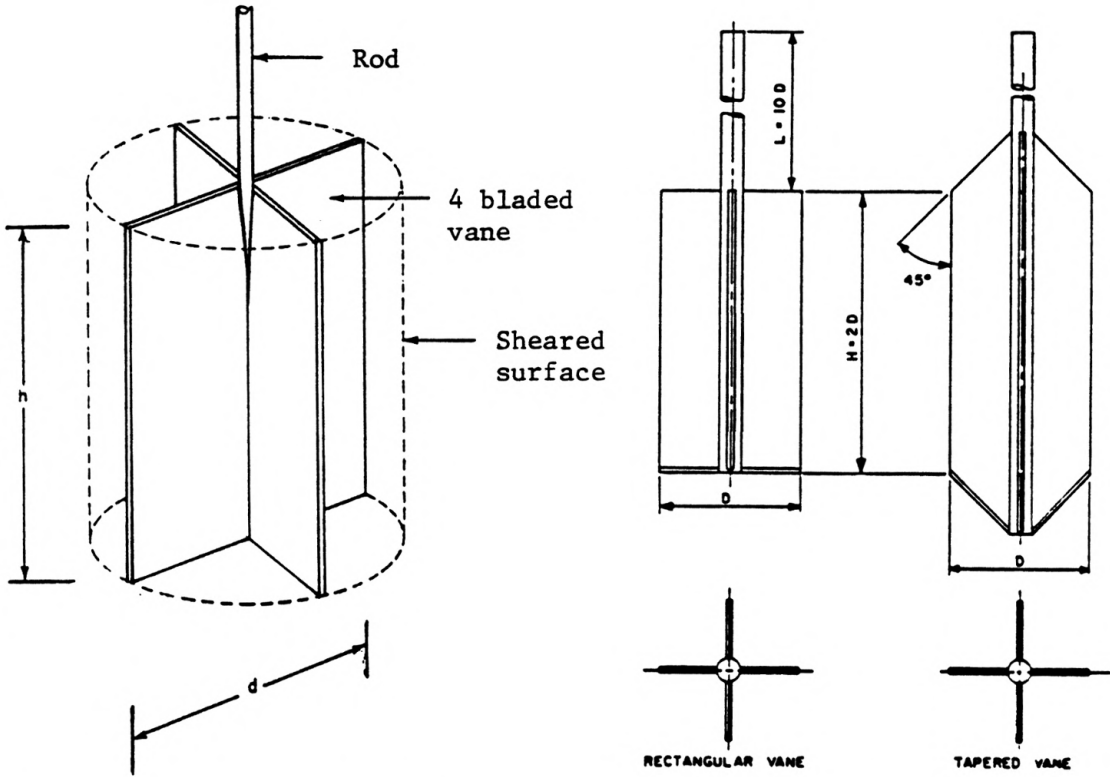


Figure 4.5 Relationship among Standard Penetration Resistance, relative density, and effective overburden pressure for coarse sand. (24)



a. Vane Shear Test Apparatus

b. Geometry of Field Vane

Figure 4.6 (13)

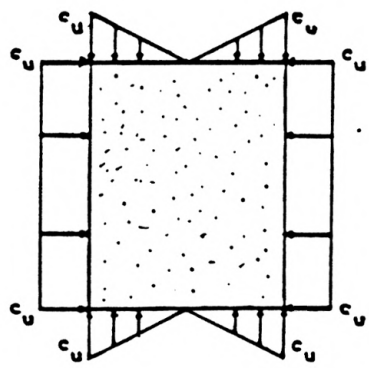


Figure 4.7 Assumed distribution of shear stress on side surface and ends of soil cylinder in the Vane Shear Test. (13)

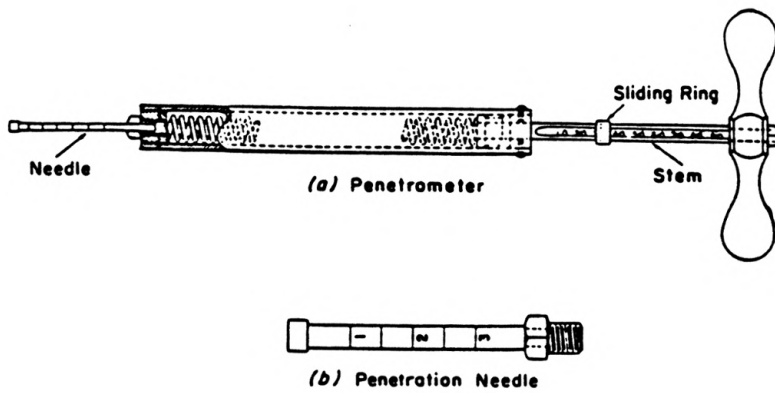


Figure 4.8 Soil Penetrometer (9)

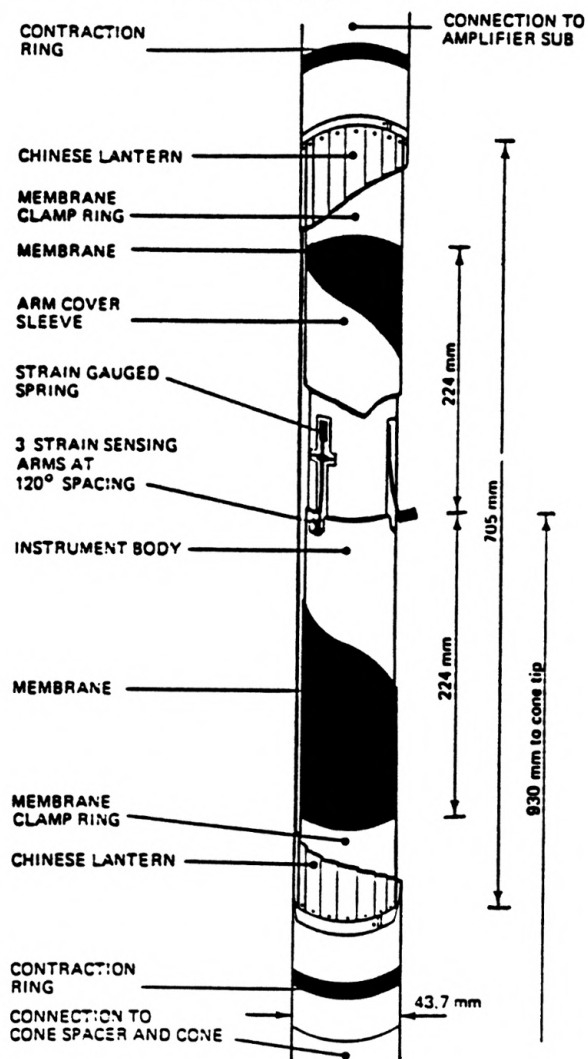


Figure 4.9 The Prototype Fugro Full Displacement Pressuremeter. (15)

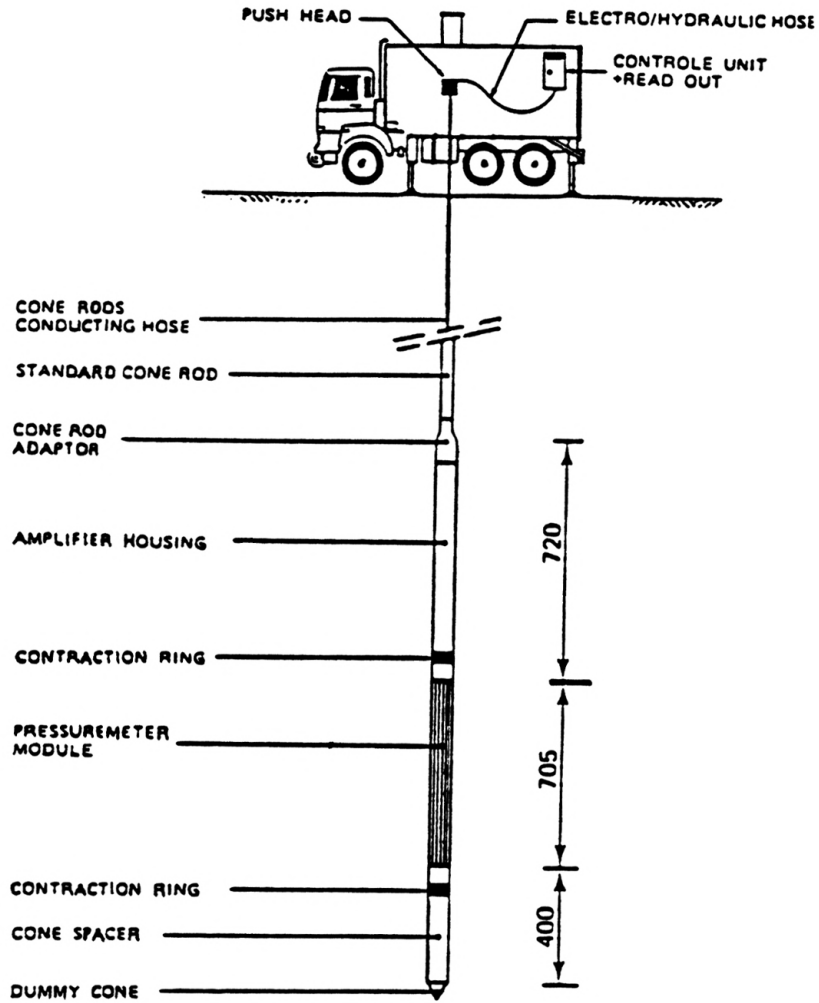


Figure 4.10 Set-up for prototype FDPM testing. (15)

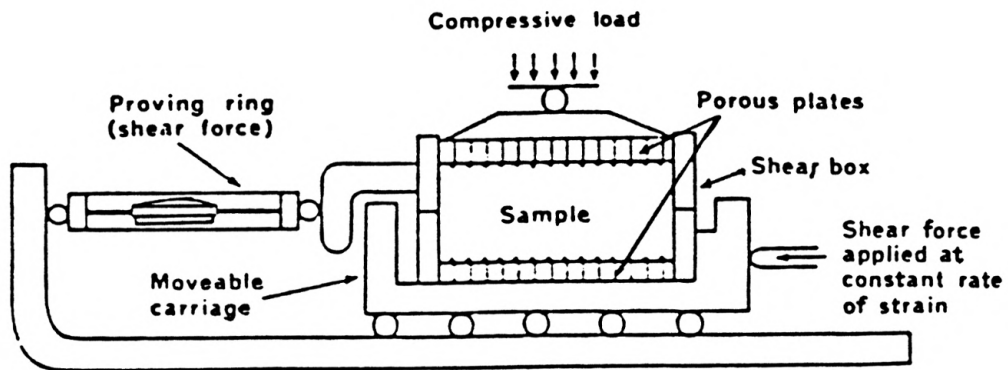


Figure 4.11 Direct Shear Stress Test Apparatus. (25)

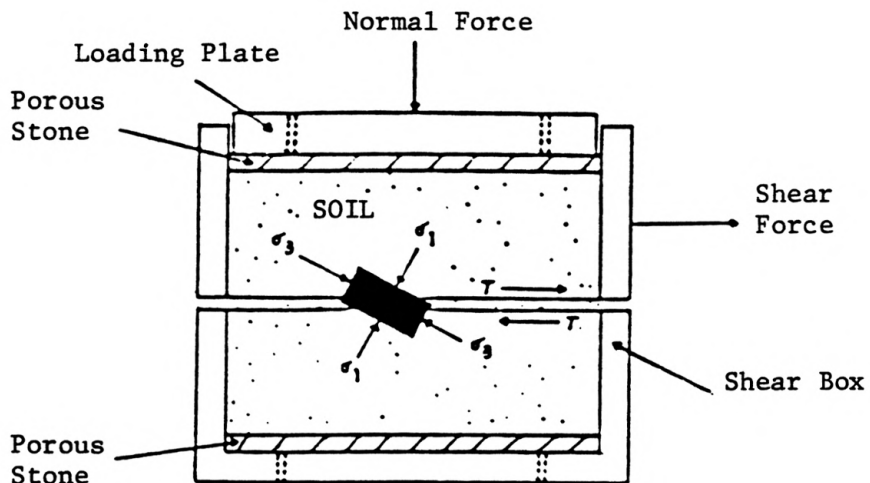
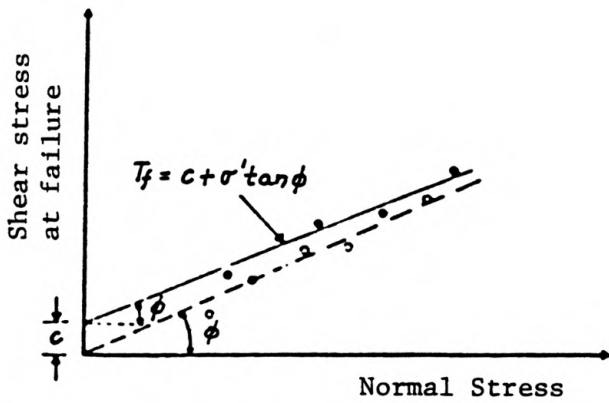


Figure 4.12 Schematic diagram of the Direct Shear Stress Test. (25)



- Tests on normally consolidated clay
  - Tests on over-consolidated clay
- Note:  $c = 0$  for normally consolidated clay;  $c > 0$  for over-consolidated clay

Figure 4.13 Failure envelope for clay obtained from the Direct Shear Test. (1).

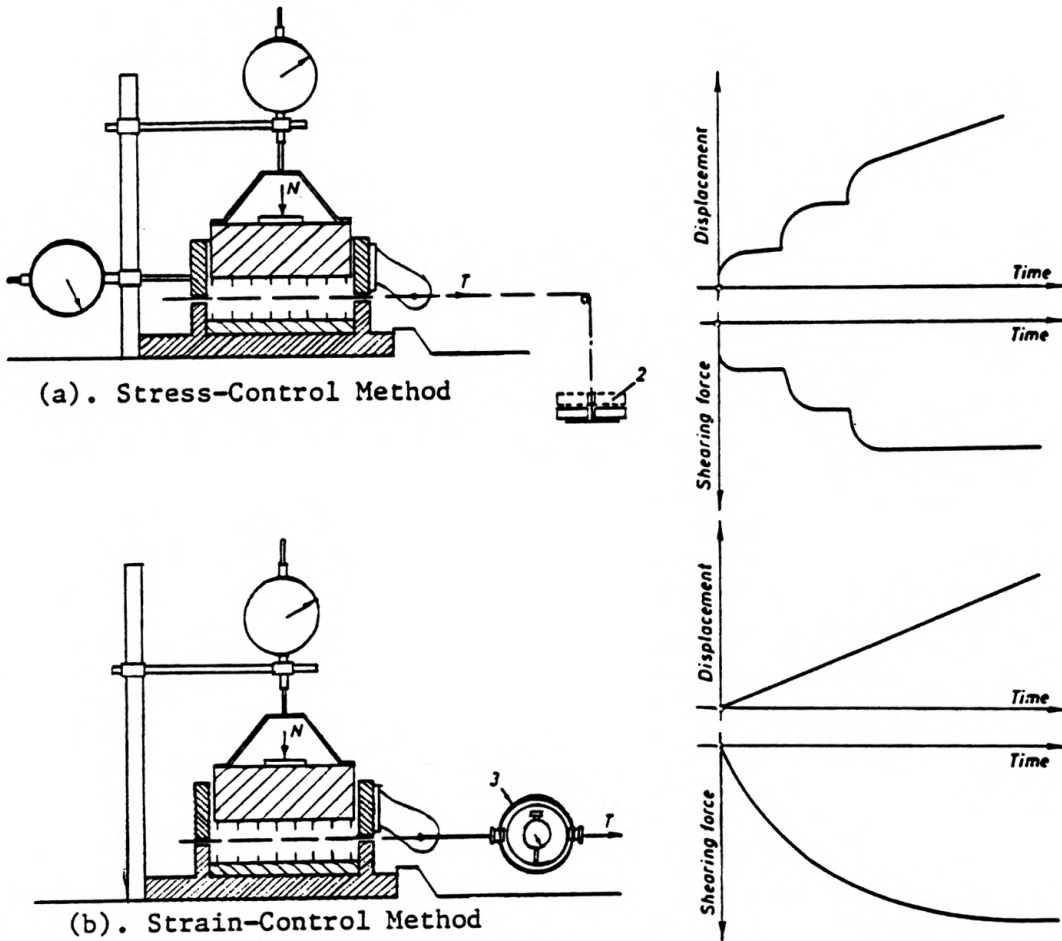


Figure 4.14 Direct Shear Test Methods. (6)

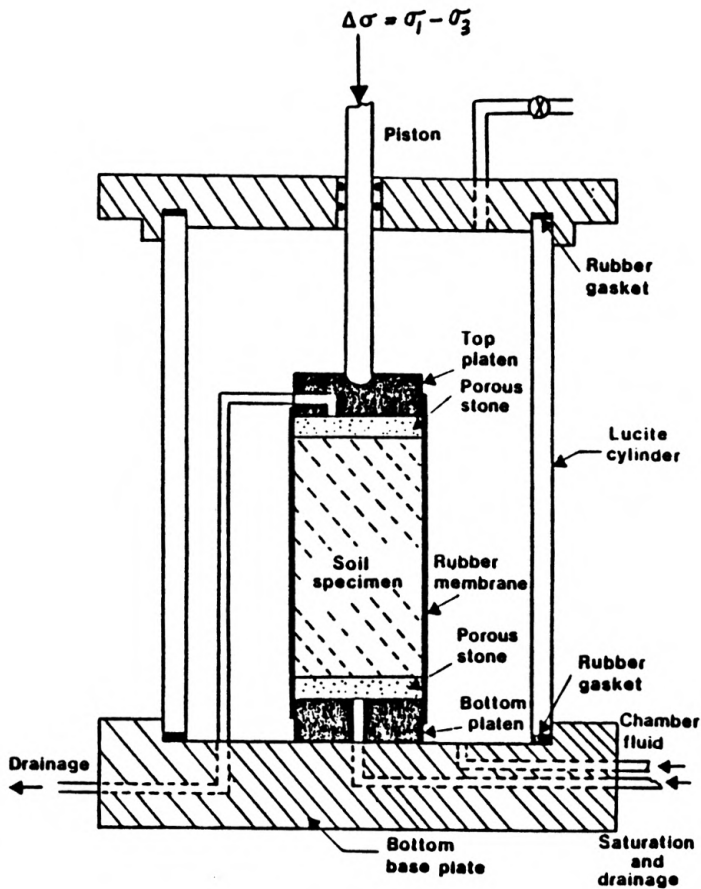


Figure 4.15 Schematic Illustration of the Triaxial Cell. (6)

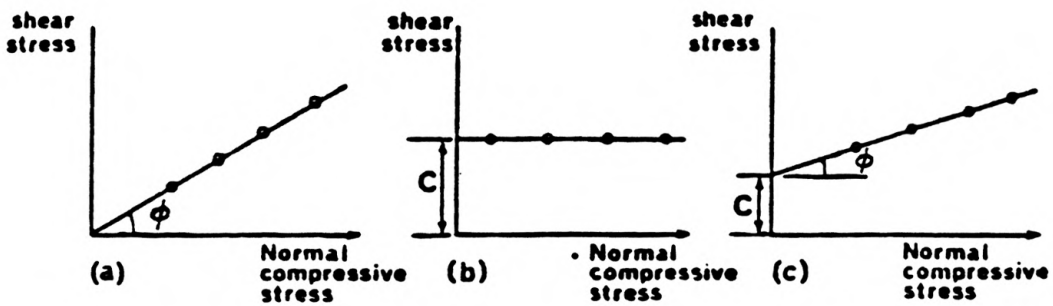


Figure 4.16 Shear Stress vs. Normal Compressive Stress relationships for the three types of soils. (24)

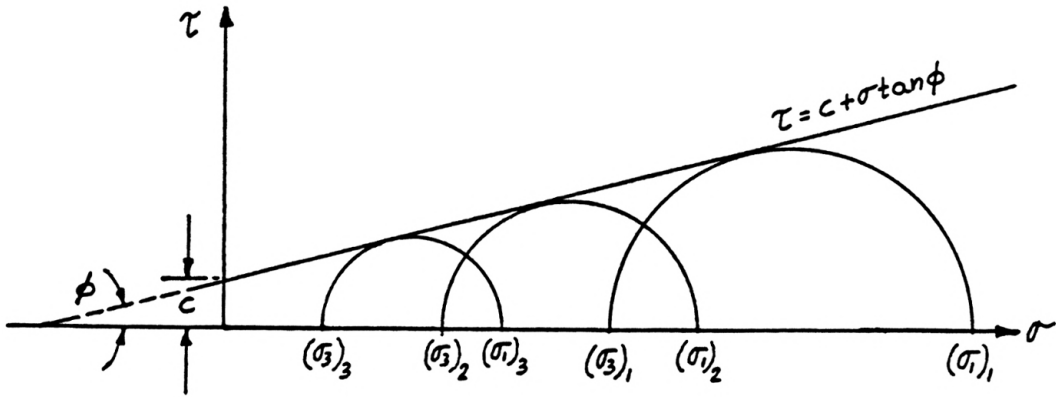


Figure 4.17 Graph of Coulomb Equation for shearing strength of soil. (24)

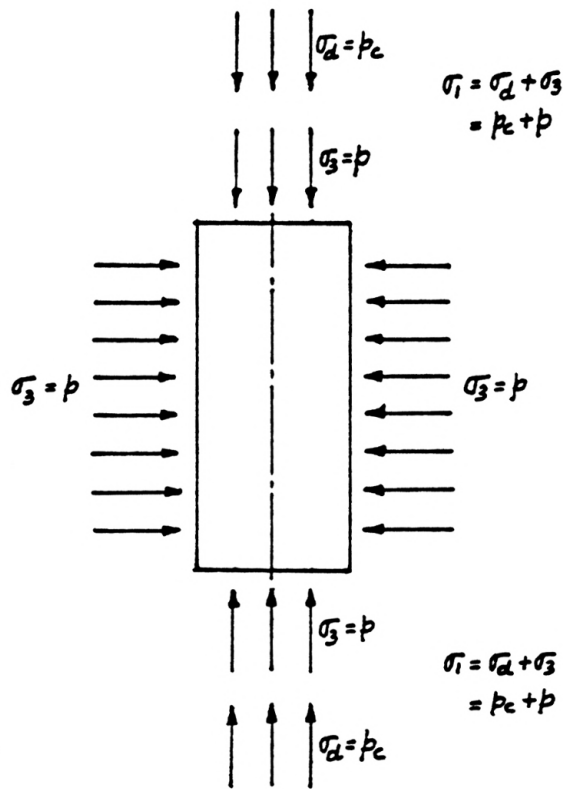
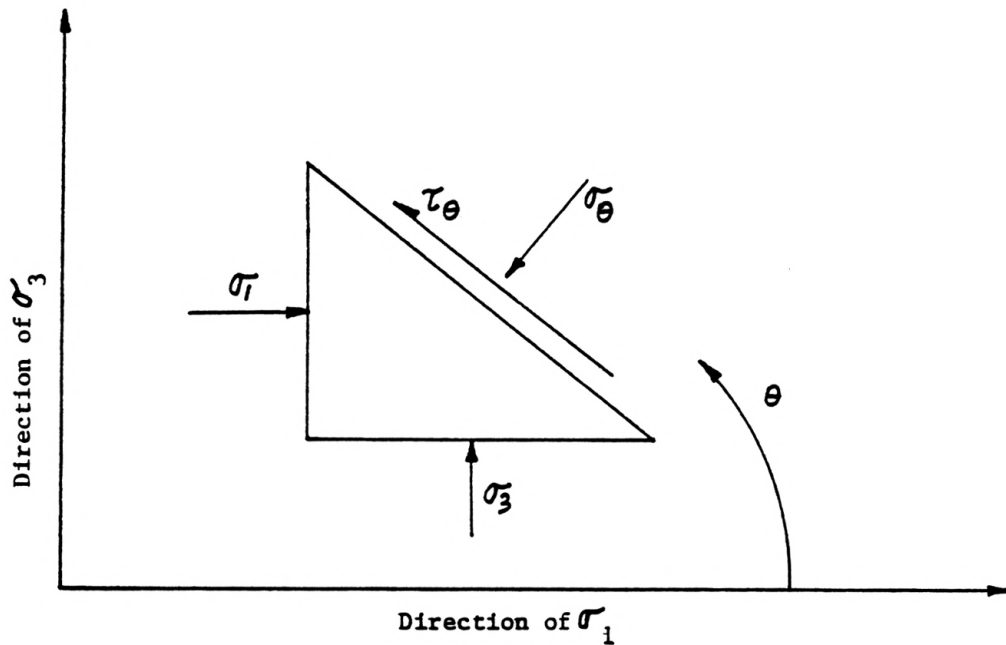
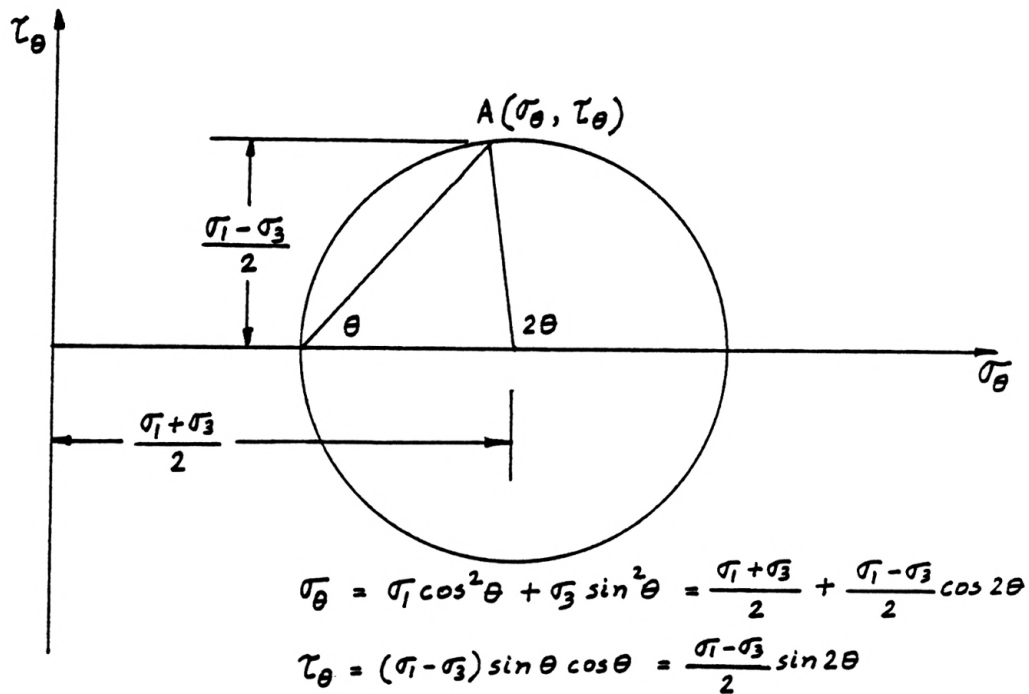


Figure 4.18 Principle of the Triaxial Compression Test. (25)



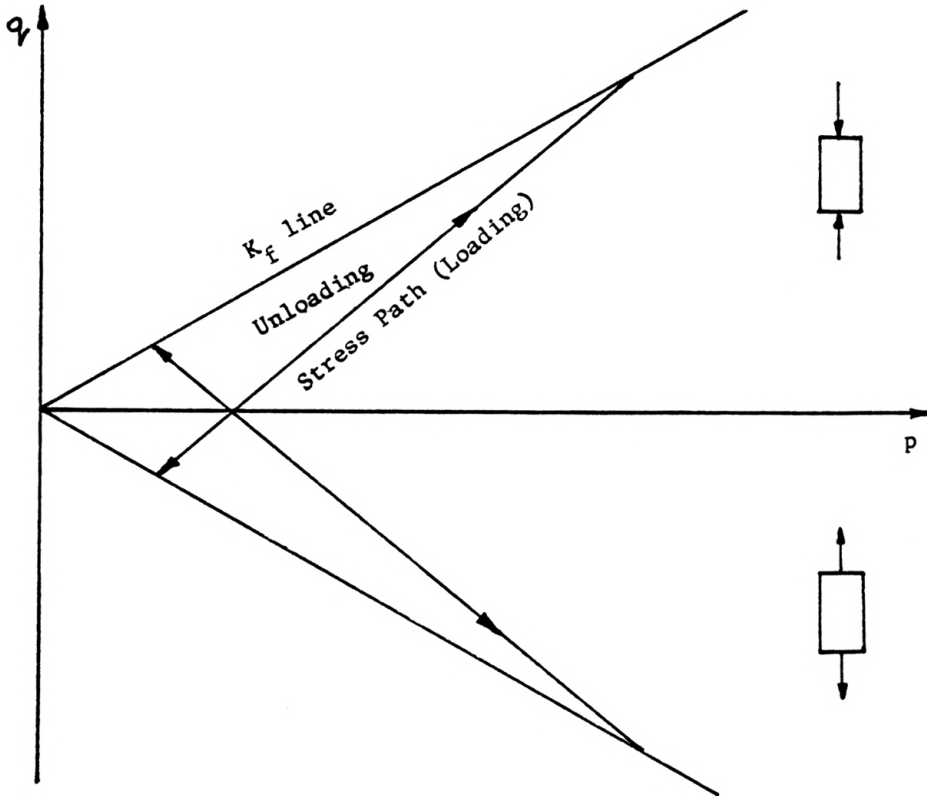


(a). Sketch showing the physical representation of a stressed sample.



(b). Sketch showing the Mohr Circle representation of the same stressed sample.

Figure 4.19 (25)



$$p = \frac{\sigma_1 + \sigma_3}{2} \quad , \quad q = \pm \frac{\sigma_1 - \sigma_3}{2}$$

Figure 4.20 Sketch showing stress representation by p and q. (25)

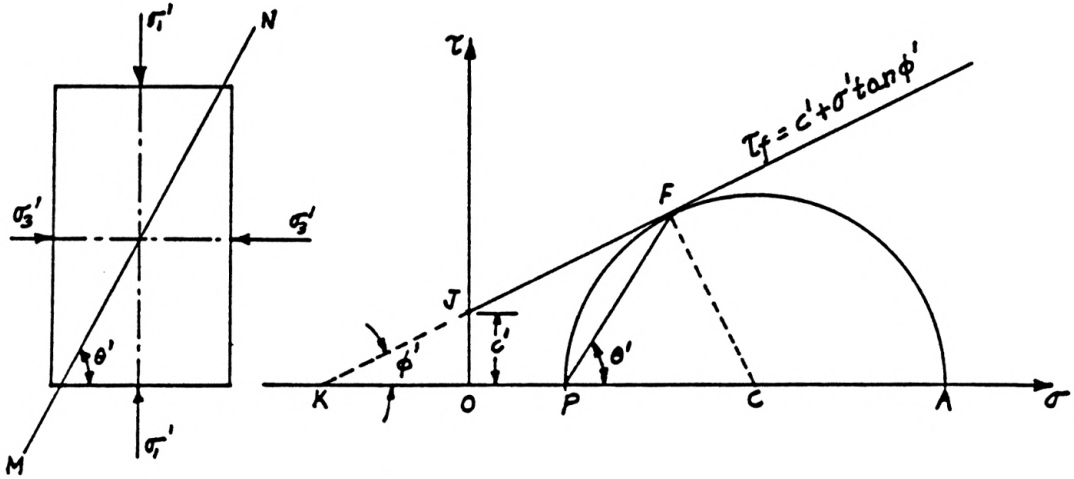


Figure 4.21 Stress condition and failure envelope generated from the Triaxial Compression Test. (25)

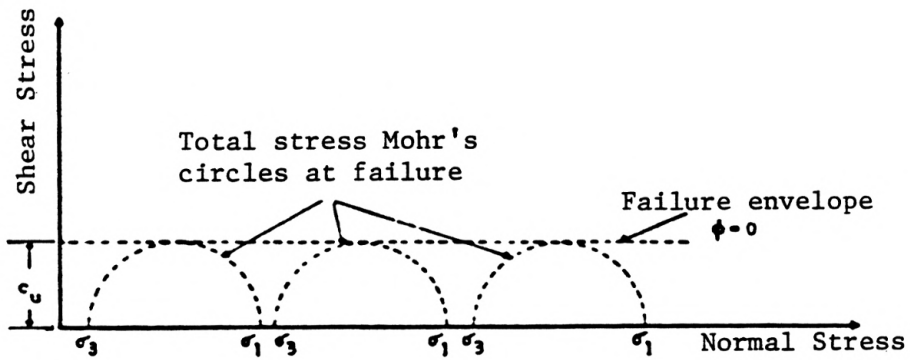


Figure 4.22 Total Stress Mohr's circles and failure envelope ( $\phi = 0$ ) obtained from unconsolidated-undrained triaxial tests. (13)

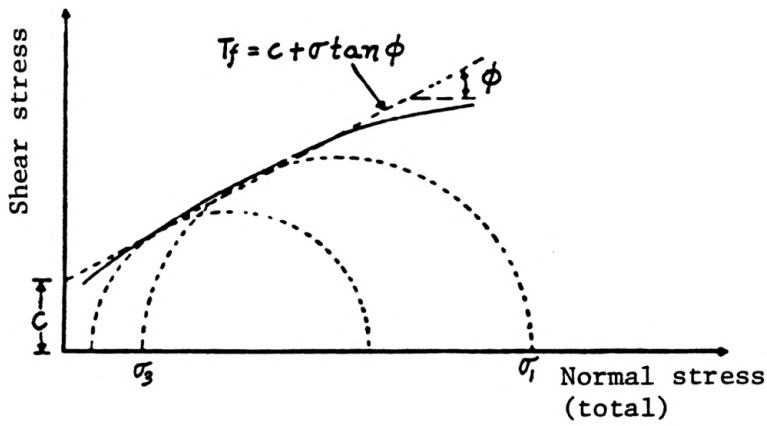


Figure 4.23 Total stress failure envelope for undrained tests on partly saturated cohesive soils. (1)

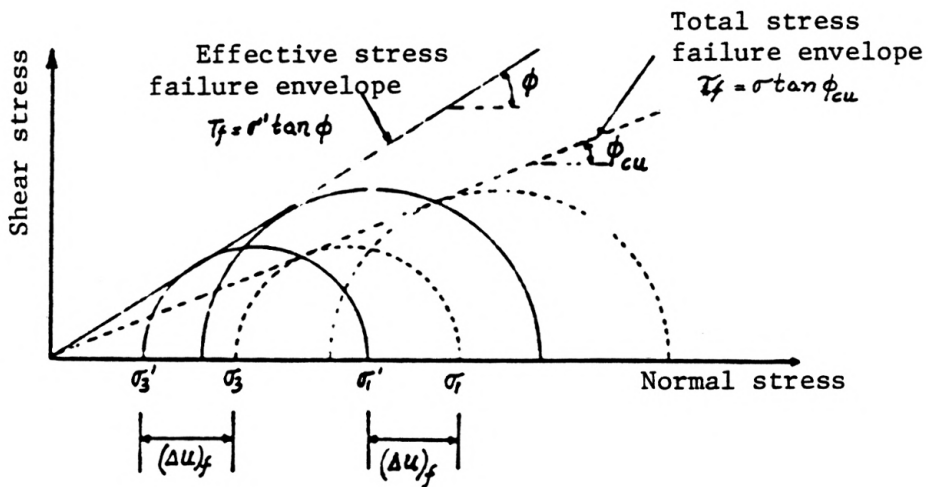


Figure 4.24 Total and effective stress failure envelope for consolidated-undrained triaxial tests. (13)

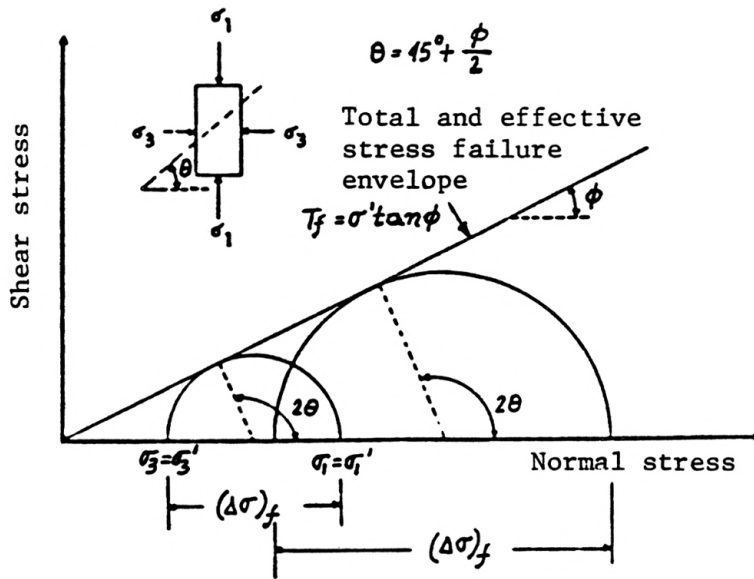


Figure 4.25 Effective stress failure envelope from drained tests in sand. (13)

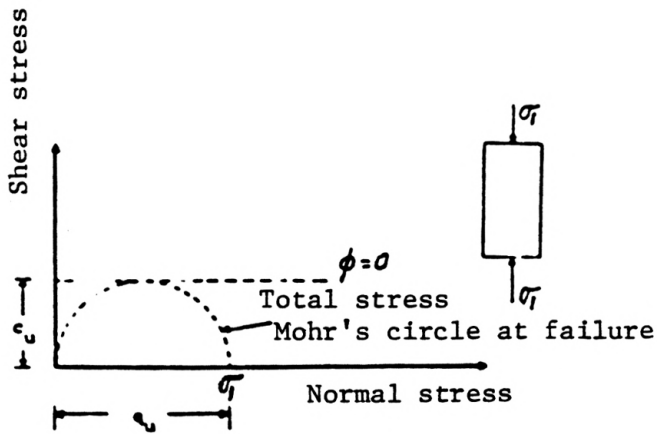


Figure 4.26 Failure envelope from Unconfined Compression Test. (25)

## CONCLUSIONS

Two basic problems exist in present-day soil analysis:

1. effect of unloading of the sample taken from depths as it is brought to the surface and removed from the sampler.
2. changes in the moisture content that may occur in the soil strata after construction is complete and the effects these changes will have on the strength of the soil.

Simplistic tests such as the Standard Penetration Test, the Vane Shear Test predict only a shear value at the conditions under which the tests are conducted.

The Direct Shear Test has its inherent disadvantages like no drainage control; the failure plane is predetermined which may not be the weakest plane; pore pressure is not measured; there is effect of lateral restraint from the side walls of the shear box.

On the other hand, the Triaxial Compression Test is the only test which incorporates control of drainage conditions and the measurement of pore pressure and is thus the most common and most reliable test for the evaluation of the stress-strain characteristics of the soil.

## BIBLIOGRAPHY

1. Bishop, A.W. and Henkel, D.J. The measurement of soil properties in the Triaxial Test., Howard Arnold Publishers Ltd., 1957.
2. Yoder, E.J. Principles of Pavement Design., John Wiley & Sons, Inc., 1959.
3. Spangler, M.G. Soil Engineering., International Textbook Company, 1951.
4. Selig, E.T. and Ladd, R.S. (Editors) Evaluation of Relative Density and its role in Geotechnical Projects involving Cohesionless Soils., American Society for Testing and Materials, 1973.
5. Kedzie, A. Handbook of Soil Mechanics: Soil Physics (Volume 1)., Elsevier Scientific Publishing Company, 1974.
6. Kedzie, A. Handbook of Soil Mechanics: Soil Testing (Volume 2)., Elsevier Scientific Publishing Company, 1980.
7. Bowles, J.E. Foundation Analysis and Design., McGraw-Hill Book Company, 1982.
8. Cernica, J.H. Geotechnical Engineering., Holt, Rinehart and Winston, CBS College Publishing, 1982.
9. Smith, G.N. Elements of Soil Mechanics for Civil and Mining Engineers., Crosby Lockwood & Sons, Ltd., 1968.
10. Scott, C.R. An Introduction to Soil Mechanics and Foundations., Maclaren and Sons, Ltd., 1969.
11. Whitlow, R. Basic Soil Mechanics., Construction Press, 1983.
12. Smith, M.J. Soil Mechanics., Macdonald and Evans, Ltd., 1970.
13. Das, B.M. Introduction to Soil Mechanics., The Iowa State University Press, Ames, 1979.

14. Tschebotarioff, G.P. Soil Mechanics, Foundation, and Earth Structures: An Introduction to Theory and Practice of Design and Construction., McGraw-Hill Book Company Inc., 1951.
15. Baguelin, F.; Jezequel, J.F.; and Shields, D.H. The Pressuremeter and Foundation Engineering, Trans Tech Publications, 1978.
16. Peck, R.B.; Hanson, W.E.; and Thornburn, T.H. Foundation Engineering, John Wiley & Sons, 1953.
17. Parker, J.C.; Amos, D.F.; Sture, S. Measurement of Swelling, Hydraulic Conductivity, and Shear Strength in a Multistage Triaxial Test; J-44:1133-1138, 1980, American Society of Soil Sciences.
18. D 1558-71(1977) Test Method for Moisture-Penetration Resistance Relations of fine-grained soils, 1984 Annual Book of ASTM Standards vol. 04.08.
19. D 1586-67(1974) Method for Penetration Test and Split Barrel Sampling of Soils, 1984 Annual Book of ASTM Standards vol. 04.08.
20. D 2166-66(1979) Test Methods for Unconfined Compression Strength of Cohesive Soils, 1984 Annual Book of ASTM Standards vol. 04.08.
21. D 2573-72(1978) Method for Vane Shear Test in Cohesive Soils, 1984 Annual Book for ASTM Standards vol. 04.08.
22. D 2850-82 Method for Unconsolidated, Undrained Compressive Strength of Cohesive Soils in Triaxial Compression, 1984 Annual Book of ASTM Standards vol. 04.08.
23. D 3080-72(1979) Method for Direct Shear Test on soils under Consolidated Drained conditions, 1984 Annual Book of ASTM Standards vol. 04.08.
24. Class Notes: Kansas State University.
25. Murthy, V.N.S. Soil Mechanics and Foundation Engineering, Dhanpat Rai & Sons, India, 1977.



## ACKNOWLEDGEMENTS

The author would like to express his deep appreciation and gratitude to Professor W. W. Williams for exposing him to the basic ideas and concepts of this report. His sincere interest and enthusiasm in this project, as well as his continuing encouragement, helped make this a tremendous learning experience.

The author also wishes to extend his gratitude and appreciation to the members of his graduate advisory committee: Dr. J. B. Sisson and Dr. B. M. McEnroe for their assistance and review of this report.

Finally, the author wishes to express his sincere appreciation and thanks to all the faculty and staff in the Civil Engineering Department at Kansas State University, for creating a very healthy environment for pursuing graduate studies.

METHODS FOR DETERMINING SHEAR STRENGTH  
OF SOILS AND THE LIMITATIONS AND/OR  
ADVANTAGES OF THE VARIOUS TESTS

by

Amit Mukherjee

B.E., Calcutta University, India, 1983



AN ABSTRACT OF A MASTER'S REPORT

submitted in partial fulfillment of the  
requirements for the degree

MASTER OF SCIENCE

Department of Civil Engineering

KANSAS STATE UNIVERSITY  
Manhattan, Kansas

1987

## ABSTRACT

The friction angle and the unit cohesion (the shear strength characteristics) of a soil are fundamental aspects in determining the suitability of soils for engineering purposes and in the analysis and design of soil-based structures.

This report consisted of studying the methods for determining the shear strength characteristics of soils and the limitations and/or the advantages of the various tests.

Amongst all the tests described, the triaxial compression test is the only one which makes it possible to investigate the change in shear strength of a soil for different ratios of major(axial) and minor(lateral) principal stresses, to control the drainage conditions during the test, and to measure the pore pressure. This test can simulate the conditions imposed on a soil mass as it exists in the field. Thus, the friction angle and the unit cohesion obtained by the use of this test approximate the true values of these properties.